UNCLASSIFIED
SECURITY CLASSIFICATION OF THIS PAGE

REPORT DOCUMENTATION PAGE	READ INSTRUCTIONS BEFORE COMPLETING FORM
1. REPORT NUMBER: AFOSR-TR- 78-1098	2. GOVT ACCESSION NO. / 3. RECIPIENT'S CATALOG NUMBER
4. TITLE (and Subtitle): IGNITION OF LIQUID FUELS IN SUPERSONIC AIR STREAMS	5. TYPE OF REPORT & PERIOD COVERED: INTERIM 1 Dec 77 - 31 Aug 78
	6. PERFORMING ORG. REPORT NUMBER: VPI-Aero-082
7. AUTHOR(s): J A SCHETZ, S C CANNON	8. CONTRACT OR GRANT NUMBER(s): AFOSR 78-3485
9. PERFORMING ORGANIZATION NAME AND ADDRESS: VIRGINIA POLYTECHNIC INSTITUTE & STATE U, AEROSPACE & OCEAN ENGINEERING DEPT, BLACKSBURG, VA 24061	10. PROGRAM ELEMENT, PROJECT, TASK AREA & WORK UNIT NUMBERS: 2308A2, 61102F
11. CONTROLLING OFFICE NAME AND ADDRESS: AIR FORCE OFFICE OF SCIENTIFICR RESEARCH/NA, BLDG 410, BOLLING AIR FORCE BASE, D C 20332	12. REPORT DATE: May 1978
	13. NUMBER OF PAGES: 78
14. MONITORING AGENCY NAME & ADDRESS(if different from Controlling Office)	15. SECURITY CLASS. (of this report): UNCLASSIFIED
	15a. DECLASSIFICATION/DOWNGRADING SCHEDULE

16. DISTRIBUTION STATEMENT (of this Report)

Approved for public release; distribution unlimited.

17. DISTRIBUTION STATEMENT (of the abstract entered in Block 20, if different from Report)

18. SUPPLEMENTARY NOTES

19. KEY WORDS (Continue on reverse side if necessary and identify by block number)
LIQUID FUELS
IGNITION
RAMJETS

20. ABSTRACT (Continue on reverse side if necessary and identify by block number)
An experimental study of the ignition of liquid fuels injected transverse to a hot supersonic (M=1.65) air stream was conducted. The liquids considered were kerosene, CS_2 and water as an inert control. The major variables were: air stagnation temperature in the range 1500 to 2300°F, injectant flow rate and injection angles from 90° to 45° upstream. The experimental observations were: temperature measurements on the wall near the injector and in the flow downstream of injection, self-luminosity photographs and infrared photographs taken with a Thermographic camera. Special attention was directed at the behavior of the liquid layer that had previously been found to form near the →

DD FORM 1 JAN 73 1473

UNCLASSIFIED
SECURITY CLASSIFICATION OF THIS PAGE (When Data Entered)

injector. No unequivocal evidence of ignition of either fuel was found for normal injection at these conditions. However, clear evidence of ignition of CS_2 was found for the upstream injection angle for $T_o \geq 2030^\circ F$ and $80 \leq P_j \leq 135$ psi. Higher injection pressures and thus high flow rates failed to produce ignition at any temperature tested. Evidence of CS_2 ignition was found in the infrared photographs and wall and in-stream temperature measurements simultaneously. The infrared photographs indicated possible ignition of the kerosene for upstream injection, but this could not be corroborated with the temperature measurements.

< or = P sub j < or =

T sub o > or =

AD A055951

AD No. ____
DDC FILE COPY

(2)

(9) AFOSR Interim Scientific Report

(14) VPI/SU-AERO-082

(11) VPI-Aero-082
May 78

(12) 80 p.

(6) IGNITION OF LIQUID FUELS IN SUPERSONIC AIR STREAMS.

(10) Joseph A. Schetz and Steven C. Cannon

Aerospace and Ocean Engineering Department

(15) AFOSR-78-3405

(16) 2304

(17) A2

(18) AFOSR

(19) TR-78-1098

This document has been approved for public release and sale; its distribution is unlimited.

DDC
RECEIVED
JUN 30 1978
F

4 06 922

78 06 27 071

Table of Contents

Nomenclature

a	moles of ethylene
b	moles of oxygen
C_{fe}	skin friction coefficient
$\dot{m}$	mass flow injectant
M	Mach number
P_{inj}	liquid injectant injection pressure
P_o	stagnation pressure
$\bar{q} \equiv \rho_j U_j^2 / \rho_e U_e^2$	momentum ratio
Q_w	wall heat transfer
S	nozzle surface distance from end of settling chamber
T	static temperature
T_e	static temperature at boundary layer edge
T_o	stagnation temperature
T_w	wall temperature away from injector
T_w'	wall temperature adjacent to injector
U	velocity
U_e	velocity at boundary layer edge
V	normal distance away from nozzle wall
δ	boundary layer thickness
$\partial F/\partial \eta$	shear in boundary layer
ρ	density

List of Figures

I. Introduction

The problems concerning spontaneous ignition and complete combustion of hyprocarbons and other fuels are very important when considering the propulsion needs of modern high-speed projectiles. Commercial concerns include safe reliable engines that are fuel efficient. Military interests, applicable for missiles and multipurpose high technology aircraft, involve engines that are not only safe, reliable and efficient but also are capable of high specific impulse and thrust output.

One solution that seems particularly well suited to the military needs, in the Mach 3 to 6 range, is the ramjet engine. In this flight regime the ramjet offers higher fuel efficiency and specific impulse than such conventional airbreathing engines as turbojets (with afterburners) and much better performance and range than rockets (non-airbreathing engines). Some drawbacks associated with the employment of ramjets are: the need for an initial acceleration system to ramjet operable velocities and present structural and material restraints encountered at the high operating temperatures and pressures (due to subsonic diffusion in the inlet).

Present solutions for the problem of initial and low acceleration are supplementary power plants for take-off, variable geometry inlets to increase the range through which the ramjet may operate and gun launching of missiles. The use of an additional engine is not desirable as this necessarily increases the weight and complexity of

the vehicle.

To alleviate the material and structural problems resulting from high temperature operation, three possible answers are being pursued. The logical first step is that of attempting to develop new materials that will withstand these high temperatures. Another concept being investigated is that of actively cooling the internal engine surfaces by ducting and circulation of a coolant, normally the fuel. Both of these methods have enjoyed only limited success. As faster and faster speeds are being sought a third alternative has received more attention, that of supersonic combustion ramjets (scramjets). The scramjet is theoretically most efficient in the Mach 8 - 10 region, but as there is no subsonic diffusion in the inlet (i.e., no normal shock) it experiences relatively lower static temperatures and pressures than the ramjet. Thus materially and structurally the engine might survive and perform up to orbital velocities (Ref. (1)).

Problems concerning scramjet development are twofold. Like the ramjet, the scramjet suffers the problem of initial acceleration and operation into the working regime of the engine. Proposed solutions to this problem are much the same as those for the ramjet. The second problem associated with scramjets is that of ignition and total combustion of the fuel. To completely understand this restraint an understanding of the nature of spontaneous ignition and the combustion process is necessary.

For our purposes, spontaneous combustion might be defined as the ignition and significant chemical reaction of hydrocarbons or other

fuels, due to the ambient conditions in the reaction chamber, with the absence of artificial high energy ignition sources (e.g., spark plugs, etc.). The reason for this being that a decrease in the reliability in the system and, in the case of supersonic combustion, a decrease in the efficiency of the combustor results from their use. From a chemist's point of view, complete combustion will occur when the ratio of the constituents of a reaction are equal to that derived in a stoichiometric equation representing the reaction, and there is sufficient energy for the exothermic reaction to initiate and proceed.

Propulsive considerations of combustion include both these ideas. The former as concerns the limits of ignition, where primary concerns include the ambient conditions for the reaction (i.e., pressure and temperature) and fuel concentration. The latter condition is desirous when fuel efficiency and thrust parameters are being considered.

At supersonic speeds both ignition and total combustion of the fuel becomes a problem. In this flight regime the inlet air to the combustor is slowed down to Mach numbers between 1.5 and 2.5. This is so much faster than the subsonic conditions in the ramjet engine, that fuel injected into the airstream requires a much longer combustor length to insure ignition and total combustion of the fuel. At these speeds the time between injection and ignition of the fuel (ignition delay) is no longer negligible. For fuels like JP-4, this ignition delay time is of the order of 10^{-2} seconds (Ref. (2)). When injected into a Mach 2.0 flow at 50,000 feet, typical velocities of 2200 ft/sec would necessitate combustor lengths of 10 to 20 feet (depending on the

momentum of the main flow and of the injectant). This means not only having to pay an extra weight penalty due to increased combustor length, but this combustor must also be insulated to reduce the heat loss along this length. The above conclusion, that an elongated combustor must be incorporated into an engine operating in such a regime constitutes the framework most engineers are using in designing prototype scramjet engines. This will offset some of the increased thrust and fuel efficiency available with scramjets over other engines for a range of Mach numbers.

One possible solution which would enable the use of shorter combustor lengths is that of using hydrogen instead fo the liquid fuels. Hydrogen can have a shorter ignition delay time, but the minimum ignition temperature is even higher than that for hydrocarbons. Additionally hydrogen is much less dense than liquid fuels, and the associated thrust parameters are less satisfactory. Hydrogen for safety reasons, must also be stored at cryogenic temperatures. The equipment needed to cool and contain the hydrogen at these temperatures would undesirably increase the weight of the vehicle.

The study of liquid fuel injection into supersonic flows, besides being of interest in scramjet research, is also directly applicable to thrust vector control in rocket nozzles and external burning on projectiles (Ref. (3)) and is of interest when considering transpiration cooling of re-entry bodies.

Much analytical work has been accomplished concerning the performance parameters for scramjet engines (e.g., Ref. (4)). Also limited experimental research has been performed (e.g., Ref. (3)). However most of these studies were not concerned with trying to minimize the ignition delay time and thus the size of the combustor. Two recent experimental investigations (Ref. (5) and (6)) have attempted to clarify this problem. Ref. (5) attacked the problem of reducing the ignition delay by increasing the stagnation temperature of the flow, thus increasing the rate of heat transfer to the fluid. Ref. (6) tried varying the discharge coefficient of the injector and injecting at various injectant to freestream momentum ratios ($\bar{q}$), based on injectant penetration, breakup and atomization as reported by Ref. (7). The desired result was to vaporize the liquid layer reported by Ref. (5). While the results of these efforts were inconclusive (Refs. (5) and (6)), they do stand as systematic studies of ignition under conditions of practical interest for ramjets.

Some of the above references and others found in a literature search are presented in Table 1, which contains details of the various investigations. One of the more interesting studies found was that of W. Trommsdorf (Ref. (11)). This represents work at the German Army Ordnance Office from 1936 to 1938. This study was on ramjet engines using carbon disulfide as the fuel, which most investigators consider using only because of its low auto-ignition temperature. Yet the

Germans produced and fired some 260 missiles using these engines. This is the earliest applied use of ramjet technology found in the literature.

The work of Billig and Co-workers (Ref. (13)) represents efforts at the Applied Physics Lab, John Hopkins University, on different fuel blends which would be attractive for supersonic combustion from a logistics point of view. All of the injections were coaxial.

The work of Mestre et.al. (Ref. (12)) was performed at the French National Office of Studies and Aeronautical Research in 1964. The experiments in this study were carried out at the highest static air temperature found in the literature. The objective was to determine the effects of the equivalence ratio on ignition delay time.

The present study continues the most recent work, that of transverse injection of liquid fuels into supersonic flows and additionally investigates oblique-upstream injection, i.e., injection at an angle counter to the main flow, based upon observations by Ref. (8). The latter studies not only indicated a recirculation region upstream of the injection port, thus permitting an increased residence time, but also a wake of more uniform injectant concentration immediately downstream of the injector than normally reported. Both of these results theoretically would reduce the distance downstream at which ignition would initiate.

There are other directions which may yield viable solutions for shortening the residence time such as pre-atomization of the fuel, as suggested by Ref. (6). However most of these ideas, if successful,

would require a more complex injection system which would be accompanied with a higher potential for failure. The goal of this study was to seek the simplest operational system and therefore the most reliable.

This experimental investigation was carried out in a specially constructed hot air facility with initial electrical resistance heating and a "dump" type pre-burner using oxygen and ethylene as the pre-burner reactants. Kerosene and carbon disulfide (CS_2) were the two fuels used in this experiment. The former is characteristically similar to JP-4 (jet fuel) and the latter has a low reported auto-ignition temperature, 248°F, as compared to that for kerosene, 469°F (Ref. (9)). These fuels were injected into a Mach 1.65 flow via a 0.030 inch diameter orifice normal to the flow and into the flow at 45° with respect to normal. Water was also injected under similar conditions to obtain base-line data for comparison with the fuel injections.

Basically three methods were employed to observe and help determine if ignition had occured. For all the runs a wall surface temperature just downstream of the injection port was measured using a thermocouple. For some runs a thermocouple was also placed in the flow downstream of the injection port and approximately 0.05 inches above the wall. Next, black and white high-speed direct luminosity photographs were taken and some particularly interesting tests were monitored with a black and white video camera. Lastly, for some runs infrared pictures, consisting of color bands representing different

temperature isotherms on the surface viewed, were taken using a thermographic camera.

The remainder of this report is divided into five sections. The next section contains theoretical calculations which were the basis for deciding further directions for experimental research. Following that are descriptions of the facilities and equipment used and the basic procedure used in testing and gathering data in the Experimental Apparatus and Test Procedure sections. The data is presented and discussed in the Results section and concluding remarks on the data and suggestions for further study and improved data collecting are contained in the Conclusion section.

II. Theoretical Calculations and Final Considerations for Experimental Testing

One phenomena encountered in recent research efforts on spontaneous combustion in supersonic flows was the appearance of a thin liquid layer in the boundary layer around the injector (Ref. (5) and Fig. 1). The conditions at the point of injection, of kerosene and CS_2, were: M = 1.8, Ts $\leq$ 1470^{o}R, Ps = 1.2 atm, normal injection and $\dot{m}$ = .026 lbm/sec. Using direct luminosity (black and white) and infrared photographs and temperature probing of the area above the liquid surface layer, some indications of combustion were reported. However, these cases weren't repeatable, and none of the indications of combustion overlapped from one method of observation to the other. Thus, on an individual basis, it could not be stated unequivocally that combustion did occur.

As no conclusive evidence of combustion was obtained, it was decided that an analytical investigation of the boundary layer was in order. The results of this study, velocity and temperature profiles and other flow properties that characterize the boundary layer, were used to determine what forces, and changes in forces, would result from changes in the stagnation temperature of the flow-which corresponded to actual cases in the tests of Refs. (5) and (6). This information was used to help determine other directions for experimental pursuit.

To accomplish this analysis, a computer program written by E. C. Anderson and C. H. Lewis, Ref. (7), was used. With inputs of pressure and temperature distributions and nozzle geometry, this program gives as output boundary layer profiles such as velocity and temperature

gradients and other flow properties. A drawing of the nozzle used in the experiments and from which the analytical analysis was based is in Fig. 2.

This program was based on the Reichardt eddy viscosity model The Van Driest model (Ref. (10)) could have been used instead but previous experience with both models indicated that one would not give more accurate information than the other and so the easiest to use was incorporated. The stagnation and wall temperature values used in this study corresponded to actual conditions in the most recent effort to obtain combustion, Ref. (6).

The predictions of flow development are presented in Figs. 3 through 5. Figure 3 shows the variation of boundary layer thickness along the nozzle for different stagnation temperatures. As expected the boundary layer thickness is shown to vary directly with temperature, but the change is small compared with the magnitude of the thickness (less than 3% at the injection point). Figures 4 and 5 show how the wall heat transfer and the skin friction at the boundary layer edge vary with location in the nozzle. These values seem to vary more with temperature than the boundary layer thickness does, but in the region of interest the differences are still no more than 3-5% of the magnitude of the quantity in question.

The next three figures are graphs of the velocity, shear and temperature gradients through the boundary layer at the injection station. Except for the temperature profile, apparently varying the stagnation temperature has negligible affect on the profiles presented herein.

Also, the temperature gradient is relatively small even at the wall where the largest differences occur.

The above results indicate that if the liquid layer is affected by temperature or velocity gradients in the boundary layer, then varying the stagnation temperature in the flow, within reasonable limits, will not likely change the forces acting on the liquid layer. However as the temperature of the flow has some effect on the boundary layer thickness, there may be an increase in the size of the liquid layer with increase in temperature of the flow. If this liquid layer figures prominently in the mechanics of ignition, then some other means may be necessary to effect a change in the liquid layer in this temperature regime.

Ref. (6) suggested that, were this liquid layer vaporized, then it would ignite, as ignition of the fuel occurs when it is in the gas phase. By decreasing the area of the injection port at the same mass flow rate an increase in $\bar{q}$ was attained, with the overall effect to be that of increasing the interaction between the main flow and the jet. But these actions not only tended to pulverize the jet but may also have reduced and even eliminated the amount of fuel in the boundary layer, which is where combustion is felt to be most favorable. The indications of ignition reported in that study appear to be attributable to purge of fuel left in the injection line.

Injection of the fuel counter to the flow on the other hand would increase jet/injectant interaction without increasing the penetration

of the fuel. Also, counter injection would not decrease the amount of fuel in the boundary layer.

III. Experimental Apparatus

A. Hot Air Facility

The temperatures necessary to similate supersonic flight at high altitudes was partially produced by a specially designed facility. This facility consisted of a long, thick walled Inconel 601 tube heated via electrical resistance, Fig. 9. The electric power was supplied by a bank of six Plasmatron PS-20 transformers producing approximately 40 kw. The entire facility was suspended from the ceiling in pendulum fashion with the nozzle rigidly supported. This allowed the pipe to expand when heated but at the same time held the nozzle in the same position for observation purposes.

The temperature of the pipe was monitored with a voltmeter as experience indicated a correlation between the voltage being supplied and the wall temperature of the Inconel tube. This proved to be very consistent. The Inconel tube was kept at or below 1800^{o}F since at the pressure supplied to the facility the resulting stress was determined to be safely under the calculated rupture stress.

The air supply came from Ingersoll-Rand type-40, 120 psi compressors (2) and was stored in a 70 cubic feet surge tank. The air from the tank was regulated by a Grove dome pressure regulator which adjusted the air pressure by comparing the stagnation pressure just upstream of the nozzle with a pre-set pressure supply from bottled air. Prior to entering the surge tank the compressed air passes through several filters and a dryer. This resulted in a contamination-free

supply of air-crucial considering the nature of this experiment.

B. Dump Combustor

The gas-fired dump combustor, or pre-burner, was used to obtain temperatures higher than 1650°F, Fig. 10. The combustor was constructed of a stainless steel tube 10.0 in. in length with a 3.0 in. outside diameter and a 0.5 in. wall thickness. The injector plate, Fig. 11, was constructed of stainless steel and was designed to inject ethylene and oxygen into the recirculation region of the combustor. Although the air temperature in the combustor was very high (around 1500°F), a spark plug was located just downstream of the injection plate to insure ignition.

The oxygen and ethylene were injected into the flow in gaseous form. The flow of each proceeded through an orifice designed to operate in a choked condition. Therefore, increasing/decreasing the pressure would increase/decrease the flow rate as long as the ratio of the pressure upstream of the orifice to the pressure it has to overcome to enter the combustion chamber is at least that corresponding to Mach 1. This system also included a nitrogen purge and a set of check valves. This insured safe, repeatable tests. The ratio of ethylene to oxygen injected into the pre-burner was determined in a stoichiometric equation whose products maintained the ratio of oxygen to combustion products and nitrogen equal to the ratio of oxygen to nitrogen found in "clean" air. The equation is:

$$aC_2H_4 + bO_2 + O_2 + 3.76N_2 = 2_aCO_2 + 2_aH_2O + (1+b-3a)O_2 + 3.76N_2$$

For our vitiated air:

$$\frac{1}{3.76} = \frac{1 + b - 3a}{3.76 + 4a}$$

The ratio of oxygen to ethylene was thus determined to be, $b/a = 4.06$.

The spark plug, which was located just downstream of the injection plate, was fired by a Franceformer ignition transformer. The spark plug operated from initial purge to full injection and through final purge.

Three thermocouples were located at the end of the combustor, radially displaced 90 degrees at the same cross-section, staggered from the centerline in increments of 1/4 in. This served as a means of monitoring the temperature profile of the flow entering the nozzle.

The temperature profiles leaving the pre-burner were found to be quite uniform; a typical case had a centerline temperature of 2250°F, 2250°F of 1/4 in. from the center and 2225°F 1/2 in. from the center. The maximum temperatures were always somewhat less than predicted by an adiabatic reaction in the pre-burner. We have crudely estimated that heat losses of about 100°F can be expected. It is felt that the high static temperature and pressure and the long chamber length combine to indicate complete combustion.

C. Nozzle

The nozzle used in this study was axisymmetrical and constructed of stainless steel. It was designed to produce a Mach number of 1.65 at the injection station, .25 inches from the end of the nozzle, Fig.

2. At this cross-section are two wall mounted (surface) thermocouples. One is located adjacent to and slightly downstream of the injection port, Fig. 12. The other thermocouple is located radially 90 degrees from the injector. Three pressure taps are located in the nozzle. The static pressure was sampled directly across from the injector and two stagnation pressures were sampled. One of these was monitored on a strip chart recorder and the other supplied the dome regulation valve with pressurized air to compare with pre-set bottled air.

D. Fuel Injector

The liquid fuel issued from a storage cylinder, pressurized with nitrogen, into the airstream via a .030 inch diameter port in the nozzle. The ports, one for normal and one for upstream injection, consisted of .0625 inch screws (appropriately drilled out) the ends of which mounted flush with the nozzle wall. The injection system incorporated a nitrogen purge and one way check valves, like the pre-burner, which assured accurate and safe operation.

The injectant flow rate was monitored with a Potter PC3-2C flow meter. At the same injection pressure and air temperature, the $\bar{q}$ for water is close to that of kerosene and the $\bar{q}$ for CS_2 is higher. An increase in the injection pressure will correspond to an increase in $\bar{q}$.

E. Automatic Operation

It was highly desirous that each run be accurately repeatable, and to this end the execution of each run was nearly all automated. Two cam type timers were used, Cramer Type 540, to control duration of pre-burner operation, fuel injection, and all purges. Additionally, all direct luminosity photographs were cam controlled. One of the cam timers was set on a 30 second cycle which controlled the pre-burner operation and the second cam timer. The second unit was set on a 12 second cycle and controlled fuel injection and operation of the Graflex camera used to take direct luminosity photographs. The timer sequences are shown in Fig. 13.

F. Instrumentation

The full complement of monitoring instrumentation includes thermocouples - both wall mounted and sheathed mean flow, pressure transducers and optical monitoring equipment - Graflex camera, video camera and thermographic camera.

The thermocouples used were of the Cromel-Alumel type. The pressure transducers were all Statham strain gauge type transducers. All the mean flow temperatures and pressure information were recorded on a Gould Brush 260-6 channel recorder. The wall temperatures were monitored on a Hewlett-Packard Model 7100B strip chart recorder (2 channels).

The direct luminosity photographs were made using an f2.9, inch diameter lense and a 4 x 5 Graflex camera using Polaroid type 57 sheet

film.

The video recording equipment consisted of a Sony AVC-3400 video camera with a 12-64 mm. f2.8 lense. The recording unit was a Sony AV-3600 EIAJ recorder and Scotch .5 inch high energy video tape was used to record the images.

The viewing path of the Graflex camera and the video camera is shown in Fig. 14.

The infrared photographs were produced utilizing a Thermovision Model 680 thermographic camera. This camera senses the infrared radiation emitted by a heated surface, processes these images internally and produces ten color, isothermal band images of the field of view on a color television screen. The temperature difference for each isotherm band as well as the range of temperatures observed are adjustable over a wide range. These tests were conducted with a camera setting of f14, sensitivity of 100 and a 6.0 percent transmittion gray filter. Photographs of the color television image were taken with a 4 x 5 Graflex camera using Polaroid type 58 sheet film.

The exact temperature represented by each isotherm band is a function of emissivity of the object being viewed and the "shape factor" of the surface involved. As these values are difficult to estimate, at best, the results cannot be labeled with exact temperature values. Nonetheless, this method can be used to qualitatively observe the flow. For example, if combustion were to occur in the area around the injector a discontinuity should appear in the isotherm bands, near the injector, with the colors in that region corresponding to higher

temperatures than the surrounding flow.

The viewing path of the thermographic camera was e same as those of the Graflex and video cameras, Fig. 14.

IV. Test Procedure

Execution of every test consisted of 3 main steps:

1. Turning on strip chart recorders and optical monitoring equipment.
2. Initiating air flow.
3. Starting cam timers which sequentially executed pre-burner operation, fuel injection and picture taking.

Prior to each test the conditions of the run to be made had to be "set up". First the ethylene and oxygen pressure, which supplied the pre-burner, were set to correspond with the temperature desired for that run. Next, the air bottle which supplied a comparison pressure was regulated so that the nozzle total pressure would be correct (65 psia). Then the nitrogen bottle which pressurizes the fuel container was adjusted to the proper pressure for that run. Lastly the switches connected to the automatic timers which control pre-burner operation, fuel injection, all purges and the graflex camera were checked to ensure that the run would proceed in the order planned.

For each test, the following were recorded from the beginning to the end of the run: the total pressure in the nozzle settling chamber, two stagnation temperatures in the nozzle settling chamber, nozzle wall temperatures adjacent and 90^{o} away from the injector and oxygen and ethylene pressures. Additionally for some runs a third stagnation temperature was monitored. For the other runs a thermocouple located

in the airstream, downstream of the nozzle, was monitored. Also for some runs (kerosene) the liquid injectant flow rate was monitored.

Prior to each day's runs a set procedure was followed to prepare the installation for usage. First the Plasmatrons used to electrically heat the facility were turned on 2 hours prior to the first run, a minimum "warm-up" time. Next, all the gas tanks used in the experiment were pressurized. These included: air bottles for comparison with the nozzle stagnation pressure, nitrogen bottles used to purge the pre-burner lines and pressurize the fuel container and purge that line, oxygen and ethylene bottles used to supply the pre-burner. After that, the strip chart and Gould Brush chart were turned on to "warm up". Next, the optical equipment used was adjusted which included refocusing the lense and inspecting any supporting equipment. Lastly the Ingersoll - Rand compressors were turned on and allowed to pump to 120 psi. This was sufficient pressure to supply 65 psi to nozzle after pressure losses through the Inconel piping.

V. Results

Tests were performed with three injectants - water, kerosene and CS_2, at temperatures from 1750°F to 2300°F and fuel pressure of 135 psi. At the highest temperatures each liquid was also injected at 300 psi and 450 psi, and the fuels were also injected at lower pressures. For kerosene, 135 psi corresponds to $\bar{q} = 2.4$ at T_o = 1870°F. The liquids were injected both normal and oblique-upstream (135°) with respect to the main flow.

Presentation of the results is divided into two sections, data on the normal injections and on the oblique-upstream injections. Both groups have wall temperature measurements and thermographic pictures (color) of the isotherms. Additionally the former group includes black and white high speed direct luminosity photographs. The latter group also has temperature measurements in the flow, approximately 1/4" downstream of the injection port, and black and white video recordings. A synopsis of the video records is presented in a third section, however the interested reader will have to discuss a personal review of this material with the Aerospace and Ocean Engineering Department at Virginia Tech, as an informative display of these records is not feasible in this report. Tabulated data e.g., stagnation pressure and temperature and wall temperatures, are presented in Table 2.

A. Normal Injection

Figure 15 compares normal injection of water and kerosene at

temperatures from 1750°F to 2260°F using direct luminosity photographs. Figure 15 also contains a direct luminosity photograph of CS_2 injected at a free stream temperature of 2140°F. The kerosene injections were made first, and, upon reviewing the results (To $\geq$ 2090°F), it was thought that ignition had occurred since the only light source for the photographs was that from the exhaust of the nozzle i.e., jet and injectant. After pictures were taken of the water and CS_2 injection, it was apparent that there must be a more reasonable explanation. Justification of these results seems to be that the injectant refracts and reflects the light emitted from the combustion of ethylene and oxygen in the pre-burner ("dump" combustor). The degree of light received is dependent on the amount of ethylene and oxygen reacting, the temperature of the flow and the injectant used (reflecting/refracting properties). The water and CS_2 were injected at the same pressure as the kerosene but, of course this corresponds to different $\bar{q}$'s.

The next figure, Figure 16, has thermographic pictures comparing kerosene injected at temperatures from 1960°F to 2200°F at 135 psi. Each color band in the picture represents a temperature range or isotherm. As explained in the "apparatus" section, the exact temperature represented by the color band is a function of several things and is thus hard to estimate, but the pictures do indicate temperature trends. The direction of temperature increase is depicted by the color scale at the bottom of each photograph, the colors on the left-hand side corresponding to cooler temperatures and the ones on the right-hand

side to hotter temperatures. The perturbation in the middle of the photographs, breaking up the general oval image, represents the injectant with the flow moving from left to right and the injection orifice being roughly located in the third isotherm from the outside at the center of the perturbation.

The most obvious difference in the pictures is that with increase in temperature of the freestream there is an increase in the portion of the wake that is measurably hotter than the room temperature as evidenced by the changing size in the black perturbation. This is to be expected, are thus no conclusions concerning combustion can be drawn at this point.

Next, Fig. 17 through 19, are for water, kerosene and CS_2 at 2150°F to 2200°F. For each injectant, tests were made at three different back pressures, 135 psi, 300 psi and 450 psi (an increase in the back pressure being assocaited with an increase in the $\overline{q}$). A casual observation indicates little difference between the water, kerosene and CS_2 injections as the photographs show similar isotherm characterization for all the tests. However a closer examination does reveal one consistent pattern. In the third isotherm from the outside in the injection area the isotherm is slightly perturbed for the kerosene and CS_2 injections, where it is relatively flat for the water injection. These tests were all made at close to the same temperature, unlike the previous set for kerosene. This might indicate ignition for the fuels or it may be an indication of cooling around the injection port for the water injection as the wall is cooler for water injections due to

the higher thermal conductivity of water above that of kerosene and CS_2. This last suggestion is also supported by traces of wall temperature records just downstream of the injection port which are presented in Fig. 20 for water, kerosene and CS_2 injected at 135 psi. Injection occurs at the point so labeled on the graph and continues for 4 seconds, where the ordinate is the wall temperature in degrees fahrenheit and the abscissa is time in seconds. Notice that the drop in temperature for the water injection is much more than that for kerosene and CS_2. Also notice that there are no large perturbations in the temperature during the kerosene and CS_2 injections which might indicate combustion. These tracings are similar to those for water, kerosene and CS_2 injected at 300 psi and 450 psi.

Tabulated data for all the normal injections appear in Table 2 as runs 1 through 20.

B. Oblique Upstream Injection

Now observations made for the oblique upstream injections at similar conditions as those for the normal injections are presented. Figure 21 through 23 are thermographic pictures of water, kerosene and CS_2 increasing in temperature from 1980°F to 2140°F. The orientation of the image in the pictures is the same as that described for earlier thermographic photographs with the flow moving from left to right and the perturbations indicating where the nozzle exhaust is exiting.

Again, as in the normal injections, the fuel runs indicate a hotter region downstream of the injection port. This is evidenced by the perturbation of more isotherms than just the white outside isotherm which characterizes the water injections.

Figures 24, 25 and 26 for water, kerosene and CS_2 at 300 psi and 450 psi contrast the injection of each liquid at different back pressures of the injectant (and thus different $\bar{q}$'s). As in the previous set, the fuel runs appear to be hotter downstream of the injection port than the water runs. However increasing the $\bar{q}$ does not have a noticeable affect on each injectant's temperature since the high and low pressure injections for each run look similar.

The first explanation for the difference between the water and fuel runs would be as before for the normal injection, that the water more effectively cools the wall down than the fuel injection. However Figs. 27 and 28 should dispel this notion. These figures are wall temperature tracings of each liquid at 300 psi and 450 psi. We can see that the differences in temperature are much smaller for these oblique-upstream injections than for the normal injections (Fig. 20). Also as before, there are no perturbations in the fuel wall temperatures during injection which would support the hypothesis that the differences in the thermographic pictures for water and the fuels might be combustion.

More positive indications of combustion, as concerns the injection of CS_2, are the wall and flow temperatures just downstream of the injection port at an injection pressure of 135 psi. Figure 29 has three

tracings of CS_2 injected at 135 psi for temperatures of 1980°F to 2130°F. For $T_{o\ ave} \geq 2030°F$ there are perturbations of the wall temperature all through the injection stage of the run. The in-flow temperatures just downstream of the injection port in Fig. 30 indicate the same thing with the perturbations beginning at 2030°F and consistently occurring at higher temperatures. This phenomena did not occur for CS_2 at higher injections pressure temperatures as was shown in Figs. 27 and 28.

Since temperature perturbations did not occur for CS_2 at high injection pressures (i.e. increased $\bar{q}$) but did for 135 psi, some runs were made injecting CS_2 at lower pressures to see if ignition corresponded to just one $\bar{q}$ or if there was a range. Figs. 31 and 32 consists of wall and in-flow temperature tracings of CS_2 injected at 80 psi and 90 psi for high air temperatures. Ignition is again evidenced here by the perturbations of temperature during the injection phase. Also, accompanying the temperature jumps for the CS_2 injection was an audible increase in the noise level.

Ignition of kerosene was not obtained for the same conditions as for CS_2. Wall temperature traces given in Fig. 33 for kerosene injection at high air temperatures show no evidence of heat release. The data in Fig. 29 wall temperature tracings for CS_2 injection negate another possible explanation for the temperature perturbation results, that for some reason the oblique upstream injection results in an unstable flow rate of the fuel. Unstable injection might occur because, at low $\bar{q}$, the injectant can have difficulty overcoming the freestream

momentum. If this had happened at lower temperatures, during a non-injection phase of this cyclic phenomena, there would be an increase in wall temperature due to absence of the fuel to cool the wall off. This was not observed to happen.

C. Video Records of Oblique-Upstream Injection

At this point it was decided that video recordings of these last sets of runs might provide further evidence of ignition of the CS_2 and possibly the kerosene. As before, water was also injected to provide a basis for comparison with the fuel injections.

Like the high speed direct luminosity photographs, the results were inconclusive. The recordings of the water injections are almost indistinguishable from those of kerosene and CS_2. This does not discount the possibility of ignition since the reflection of the reaction from the pre-burner may be greater than that for small amounts of combustion, which may be occurring with the fuels. Also as these recordings were in black and white they do not reflect possible differences in the intensity of the light emanating from the jet that color pictures might.

VI. Conclusion

Water, kercsene and carbon disulfide were injected both normal and oblique with respect to the main flow at various stagnation temperatures and injection pressures. Results consisting of temperature measurements and photographic records in both the visible and infrared wavelength spectrums were taken.

For the normal injection, at temperatures up to 2260°F, little evidence of combustion was found for either the kerosene or CS_2. The thermographic photographs did indicate a consistent difference between the fuel injection and the water injection, but this difference, a slight perturbation in the temperature around the injection port, was small and not corroborated with any other indications of ignition (e.g., temperature perturbations in either the wall or freestream temperature records). The best explanation for this seems to be that all the fuel in the boundary layer, where ignition is most probable, is in the liquid phase. This interpretation is supported by the results of the analytical investigation performed prior to the experimental work. The results showed that changes in the freestream stagnation temperature, and therefore the static temperature, have negligible effect on the viscous forces in the boundary layer. Thus, the liquid layer would not be expected to change radically in character with change in temperature. As a liquid it would take a larger heat transfer rate and a longer period of time for ignition to occur.

For the oblique-upstream injection cases, ignition occurred for CS_2 at $T_o \geq 2030°F$ and possibly for kerosene. These conclusions are based on thermographic photographs for the kerosene injection and thermographic photographs and wall and freestream temperature measurements for CS_2 injections. The thermographic photographs for the oblique-upstream injection of the fuels showed the same perturbations as in the normal injection, but the differences between the fuel and water injections were more exaggerated. Since the temperatures recorded at the wall were nearly the same for all the injectants (except for the CS_2 when the temperature fluctuations occurred), the differences in the thermographic photographs can not be explained as readily by increased cooling at the wall with water over the fuels. Also for the CS_2 injection, ignition is substantiated by wall and freestream temperature recordings which show temperature increase fluctuations for $T_o \geq 2030°F$. This situation was not found for CS_2 at increased injection pressures (and hence $\bar{q}$) but did reoccur for lower injection pressures ($0 \leq \bar{q} \leq 2.4$). Though the temperatures recorded when ignition was in evidence was not as high as expected, the ignition was unstable indicating that much of the heat of combustion may have gone to vaporizing the rest of the fuel injected.

Ignition seems to be more plausible for the oblique injection than the normal injection because of several characteristic of oblique injection reported in Ref. (3). The assets of oblique injection include: increased residence time of the fuel, more uniform

consistency of the resulting wake (i.e., no lean or rich areas but in fact a more vitiated plume), and improved interaction of the injectant with the freestream-due to the fuel being injected counter to the flow.

Three changes in the present system are seen as potentially increasing and controlling combustion. There is most likely an optimum angle, possibly different for each fuel, at which the fuel will burn most consistently. Thus, a systematic investigation of the angle of injection is in order. Also, pre-heating of the fuel before injection may decrease the heat transfer from the main flow necessary to initiate combustion and at the same time make the injectant easier to atomize, consequently reducing the time to combustion (ignition delay). Finally, a judicious selection of fuel blends may result in an injectant with desirable ignition properties such as low spontaneous combustion temperature and a high heat transfer coefficent.

As the thermographic photographs and the wall temperature probe did not always concurrently give evidence of ignition, some further means of detecting combustion is necessary. Two fairly uncomplicated methods which may provide more conclusive proof of combustion are the use of high speed color photographs to monitor injection and a gas sampler which might correlate the exhaust from the nozzle with theoretical products of combustion for the fuels.

References

1. Valenti, A. M., Molder, S. and Salter, G. R., "Gun-launching Supersonic Combustion Ramjets," Astronautics and Aerospace Engineering, December 1963, pp. 24-29.

2. Bunt, E. A., McMurray, G. S. and Dugger, G. L., "Ramjet Technology-Chapter 9 Combustor Design," Technical Memorandum TG 610-9, Applied Physics Lab., John Hopkins University, April 1972.

3. Dugger, G. L., "Recent Advances in Ramjet Combustion," ARS Journal, November 1959, pp. 819-827.

4. Dugger, G. L., "Comparison of Hypersonic Ramjet Engines with Subsonic and Supersonic Combustion," Fourth AGARD Combustion and Propulsion Colloquium, Milan, Italy, April 4, 1960.

5. McVey, W. J. and Schetz, J. A., "Flowfield Near Liquid Fuel Jets Injected Transverse to a Hot Supersonic Air Stream", AIAA Paper No. 75-1230, Oct. 1975.

6. Berbenti, C. and Schetz, J. A., "Experiments on Combustion of Liquid Fuel Jets," VPI-Aero-054, Virginia Polytechnic Institute, Blacksburg, Va., August 1976.

7. Joshi, P. B. and Schetz, J. A., "Effect of Injector Geometry on Characteristics of a Liquid Jet, Injected Normal to a Supersonic Airstream," AIAA Paper No. 74-1156, Oct. 1974.

8. Baranovsky, S. and Schetz, J. A., "Experimental Investigation of Liquid Fuel Injection from the Top of a Strut," presented at the Virginia Academy of Science Meeting, Blacksburg, VA., May 1978.

9. Scott, G. S., Jones, G. W. and Scott, F. E., "Determination of Ignition Temperatures of Combustible Liquids and Gases," Analytical Chemistry, Vol. 20, No. 3, March 1948.

10. White, F. M., Viscous Fluid Flow, McGraw-Hill Book Company, 1974, pp. 474-477.

11. Trommsdorff, W., "High-Velocity Free-Flying Ram-Jet Units (TR-Missiles)", History of German Guided Missiles Development, Verlay E. Appehans & Co., Brunswick, Germany.

12. Mestre, A. and Viaud, L., "Combustion Supersonique Dans Un Canal Cylindrique." Supersonic Flow Chemical Processes and Radiative Transfer, The Macmillan Company, New York, 1964.

13. Pirkle, J. C., Rice, J. L and Billig, F. S., "Scramjet Fuels Research," Quarterly Reports on Scramjet Propulsion Research to USAF(AFAPL), October 1968 - September 1969.

14. Billig, F. S., Personal Correspondence, April 1978.

15. Mullins, B. P., "Spontaneous Ignition of Fuels Injected into a Hot Air Stream", Fuel, Vol. 32, No. 2, April 1953.

TABLES

Table 1: Ignition* of Liquid Ramjet/Scramjet Fuels in High Speed Airstreams

Date	Author	Ref.	Fuel	Mach	T_s (°R)	P_s (atm)	Injection Angle	Ignition	Remarks
1936	Tronnsdorf	11	CS_2	.7 **	1150**	12.9**	90°	Yes	First Application Found in Literature
1953	Mullins	15	Kerosene	.25**	1930	1	?	Yes	$\tau = 5 \times 10^{-3}$ sec.
1964	Mastre	12	Kerosene	2.48	2146	.277	90°	Yes	Eqiv. ratio, $\phi = .55$
1968	Pirkle	13	JP-6	.75	1300	1.36**	0	No	Coaxial, $\tau = 1.5 \times 10^{-3}$ sec.
1969	Pirkle	13	HiCal 3-D	.66-.87**	1475	1	0	Yes	Coaxial, $\tau = .3 \times 10^{-3}$ sec.
1969	Pirkle	13	HiCal 3-D	1.6	1170	1	0	No	Coaxial
1969	Pirkle	13	Pentaborane	1.6	1170	1	0	Yes	Coaxial, $\tau = .19 \times 10^{-3}$ sec.
1969	Pirkle	13	HiCal 3-D	1.61	1300	1	0	Yes	Coaxial, $\tau = .31$ sec.
1976	McVey	5	Kerosene	1.8	1455**	1.2	90°	No	Inconsistent Data
1976	McVey	5	CS_2	1.8	1470**	1.2	90°	No	Inconsistent Data
1976	Berbente	6	Kerosene	1.8	1455**	1.2	90°	?	Varied P_{inj}/P_o and C_D. Data Not Conclusive
1978	Present	-	Kerosene	1.65	1720**	1	90°	No	
1978	Present	-	CS_2	1.65	1720**	1	90°	No	
1978	Present	-	Kerosene	1.65	1755**	1	135°	?	Data Supportive But Not Conclusive
1978	Present	-	CS_2	1.65	1610**	1	135°	Yes	

* Ignition defined as $\tau \leq 10^{-2}$ sec.
** Estimated Values

Table 2: Test Conditions Investigated

Test No.	Average T_o in Settling Chamber °F	T_w '°F	T_w °F	Injectant Pressure psi		
				Kerosene	CS_2	H_2O
1	1770	400	700			135
2	2080	520	690			135
3	2240	520	650			135
4	1750	500	580	135		
5	2090	710	800	135		
6	2260	690	820	135		
7	2140	650	830		135	
8	1960	610	790	135		
9	2110	680	910	135		
10	2200	700	960	135		
11	2050	641	930	135		
12	2200	220	990			450
13	2200	340	970			300
14	2200	420	900			135
15	2150	730	990	450		
16	2150	710	1010	300		
17	2150	650	880	135		
18	2200	730	890		450	
19	2200	760	900		300	
20	2200	780	950		135	
21	2010	140	860			135
22	2040	140	880			135
23	2100	140	890			135
24	2010	240	840	135		
25	2040	240	870	135		
26	2140	250	950	135		
27	1980	100	940		135	

Table 2: Test Conditions Investigated (continued)

Test No.	Average T_o in Settling Chamber °F	T_w' °F	T_w °F	Injectant Pressure psi		
				Kerosene	CS_2	H_2O
28	2030	120	920		135	
29	2130	120	980		135	
30	2290	150	900			300
31	2260	150	980			450
32	2240	230	920	300		
33	2250	240	970	450		
34	2210	100	990		300	
35	2210	110	1000		450	
36	2210	410	970		80	
37	2200	100	910		90	

FIGURES

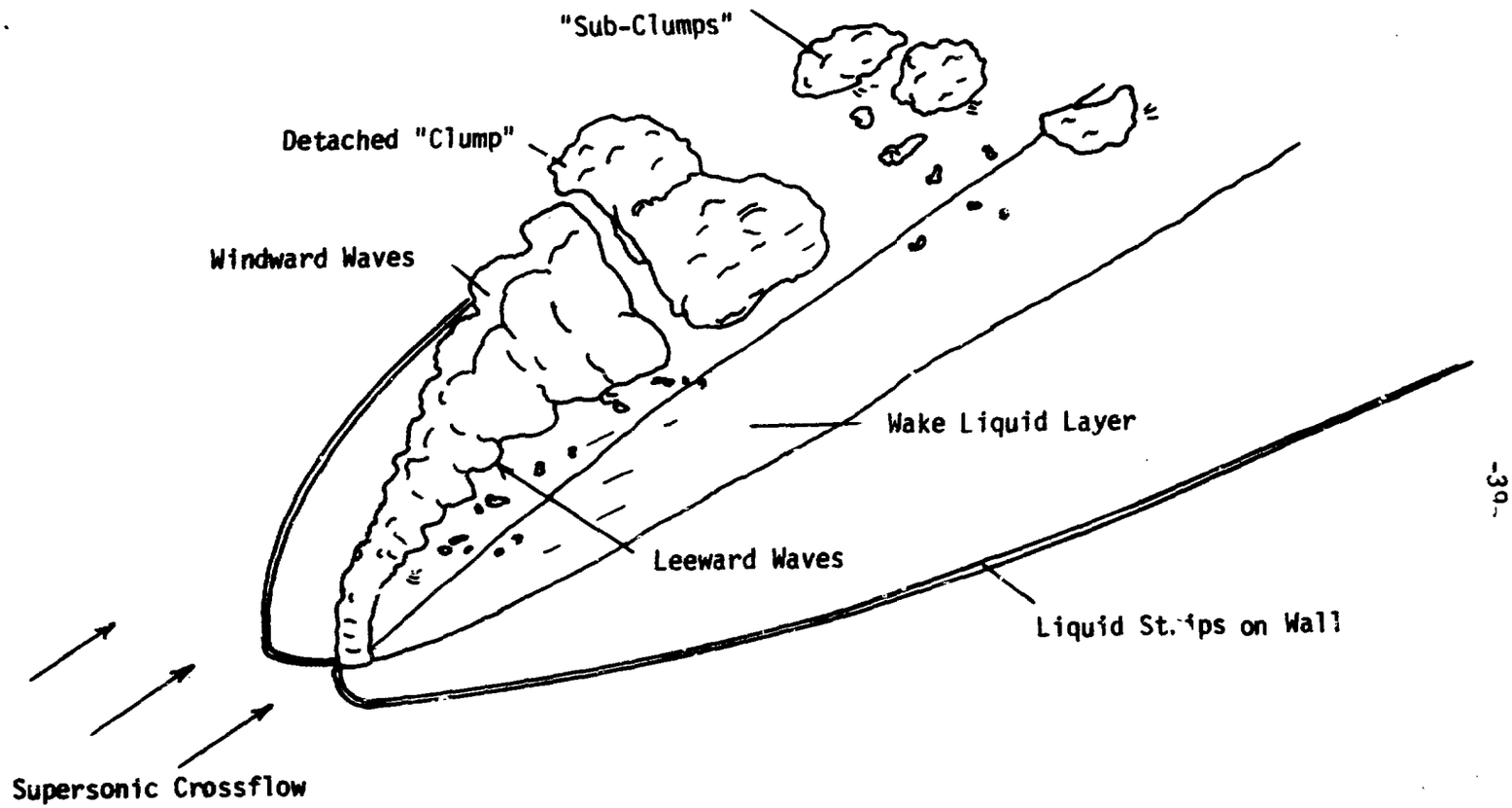

Figure 1: Isometric Sketch of Plume with Liquid Layer

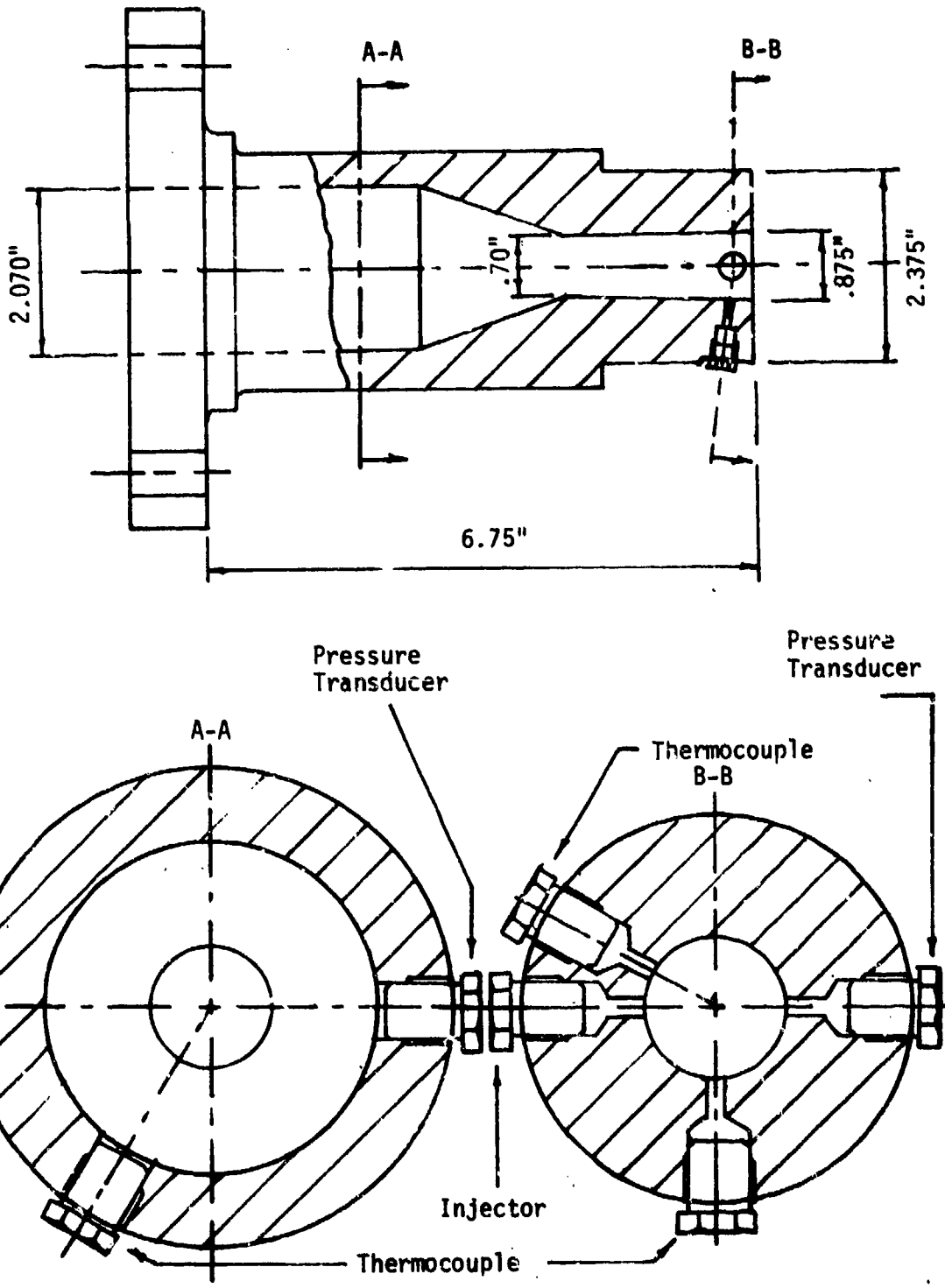

Figure 2: Test Nozzle

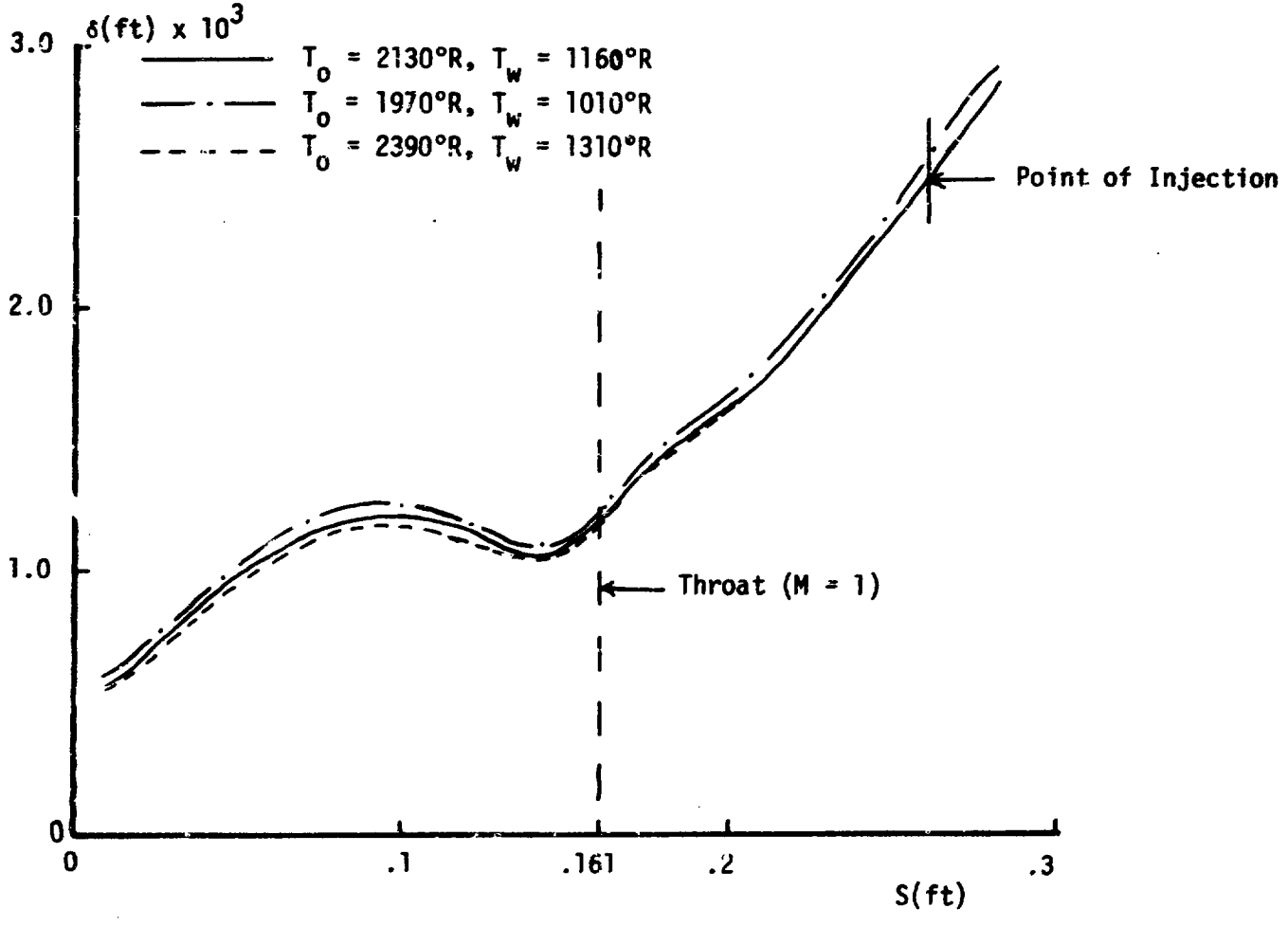

Figure 3: Boundary Layer Thickness Versus Surface Distance from Leading Edge of Nozzle

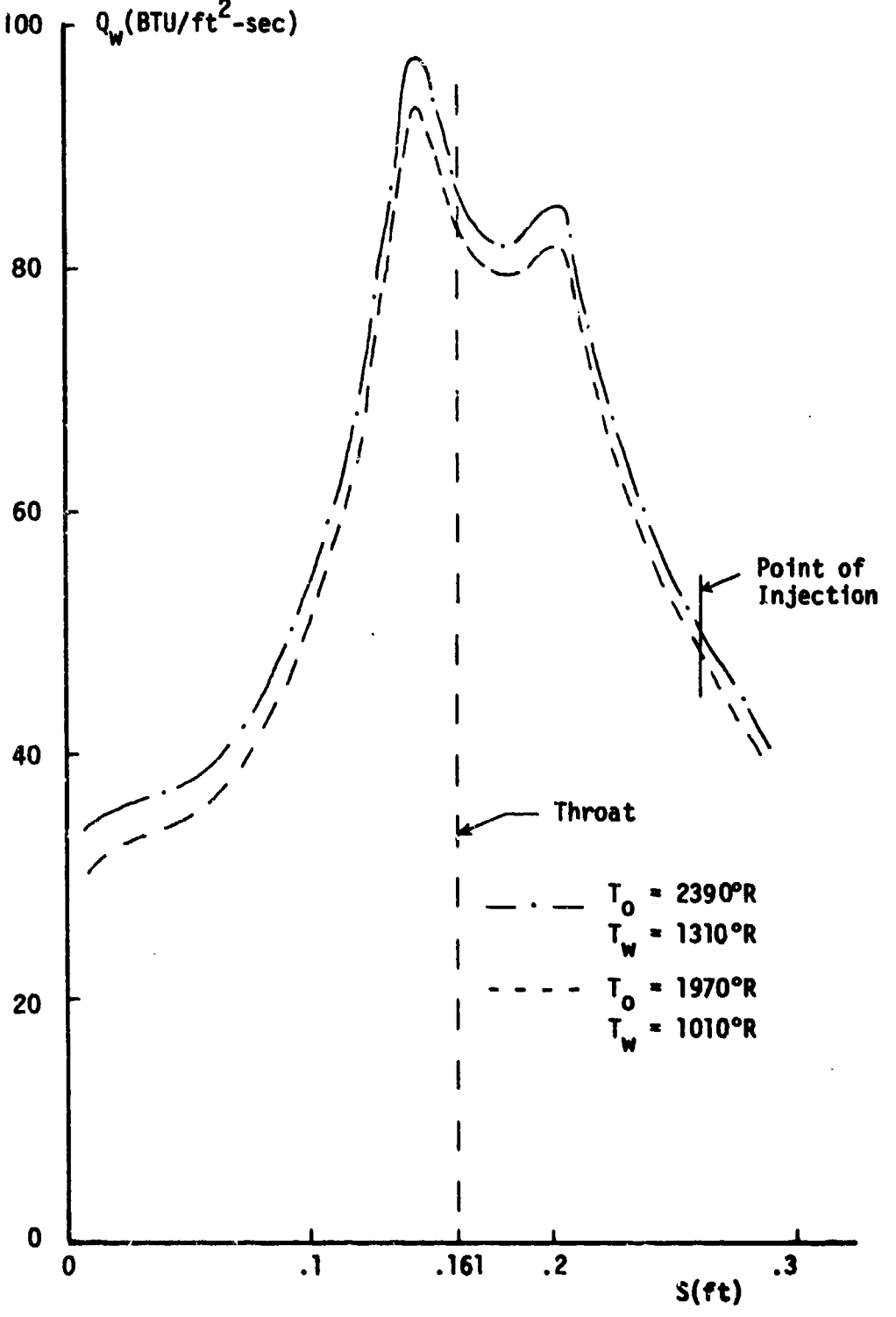

Figure 4: Wall Heat Transfer Versus Surface Distance

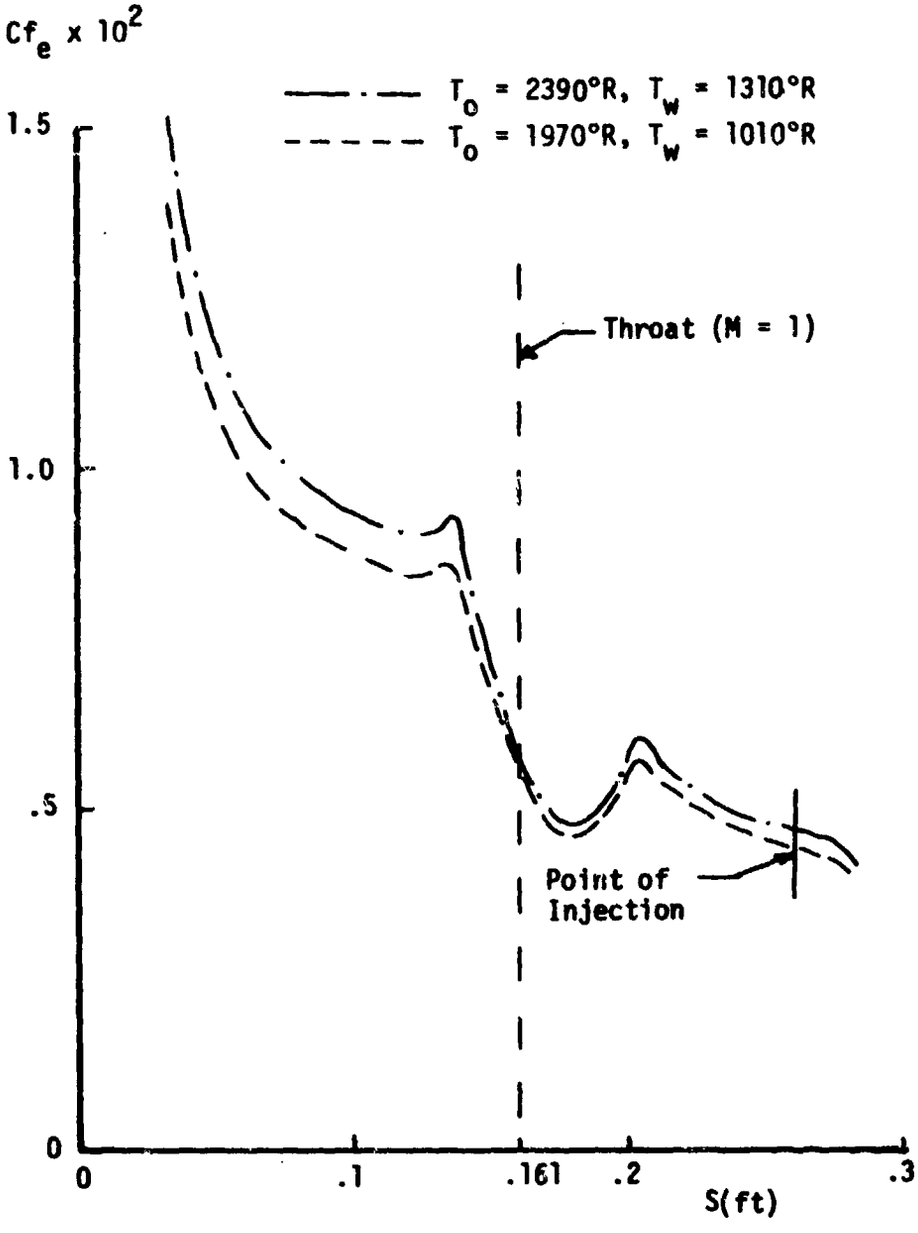

Figure 5: Skin Friction Coefficient as a Function on the Distance from the Leading Edge of the Nozzle

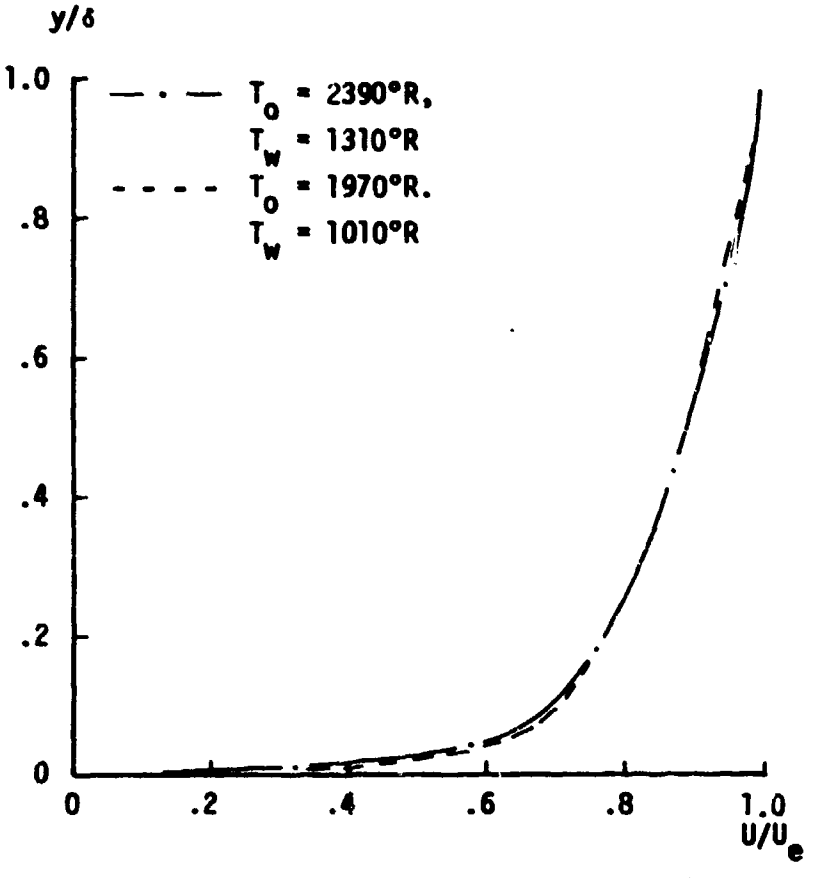

Figure 6: Boundary Layer Profile at Injection Station

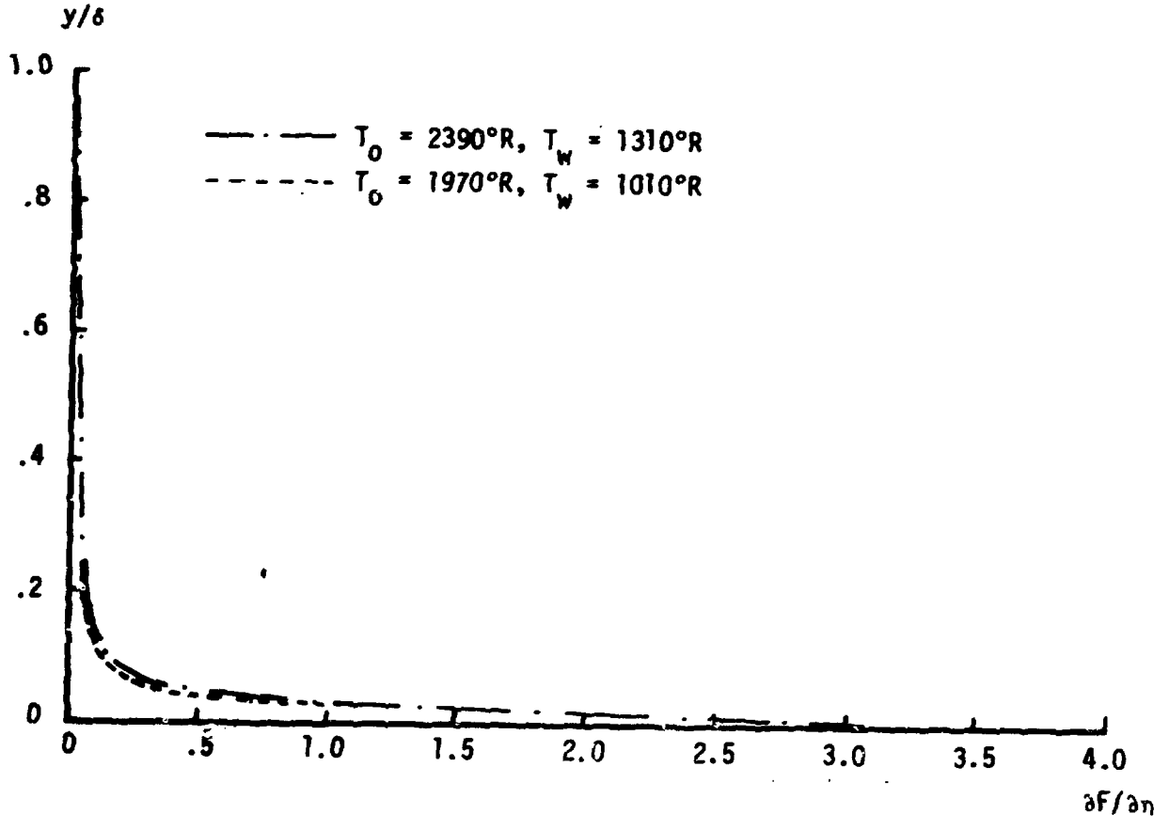

Figure 7: Shear Profile in the Boundary Layer at Injection Station

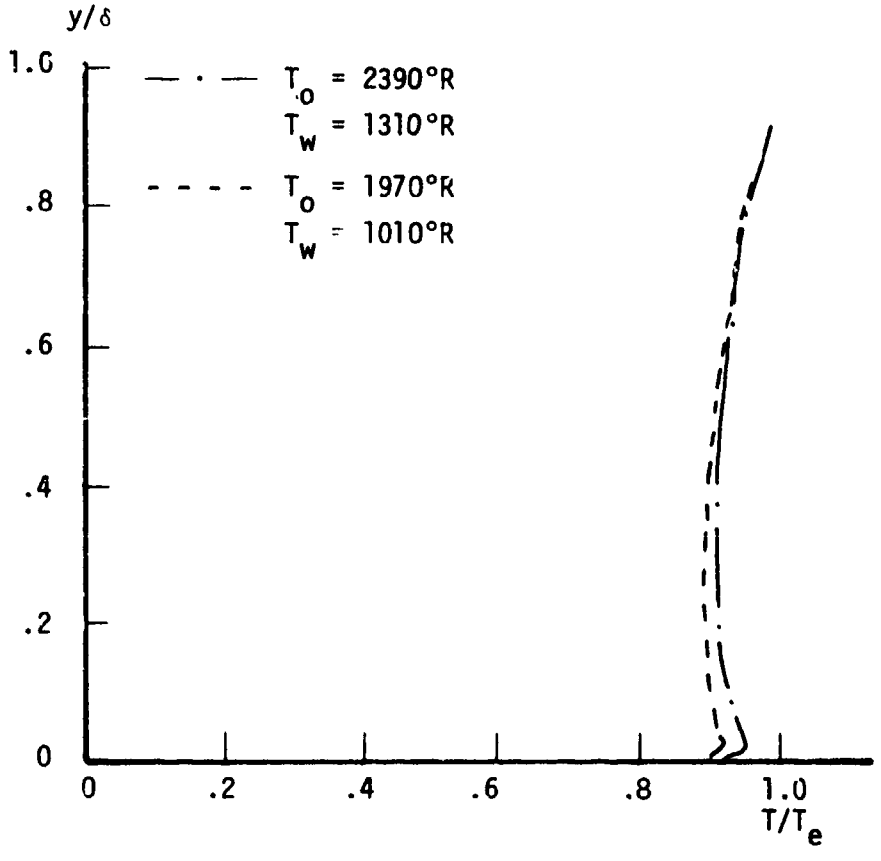

Figure 8: Temperature Profile in the Boundary Layer at Injection Station

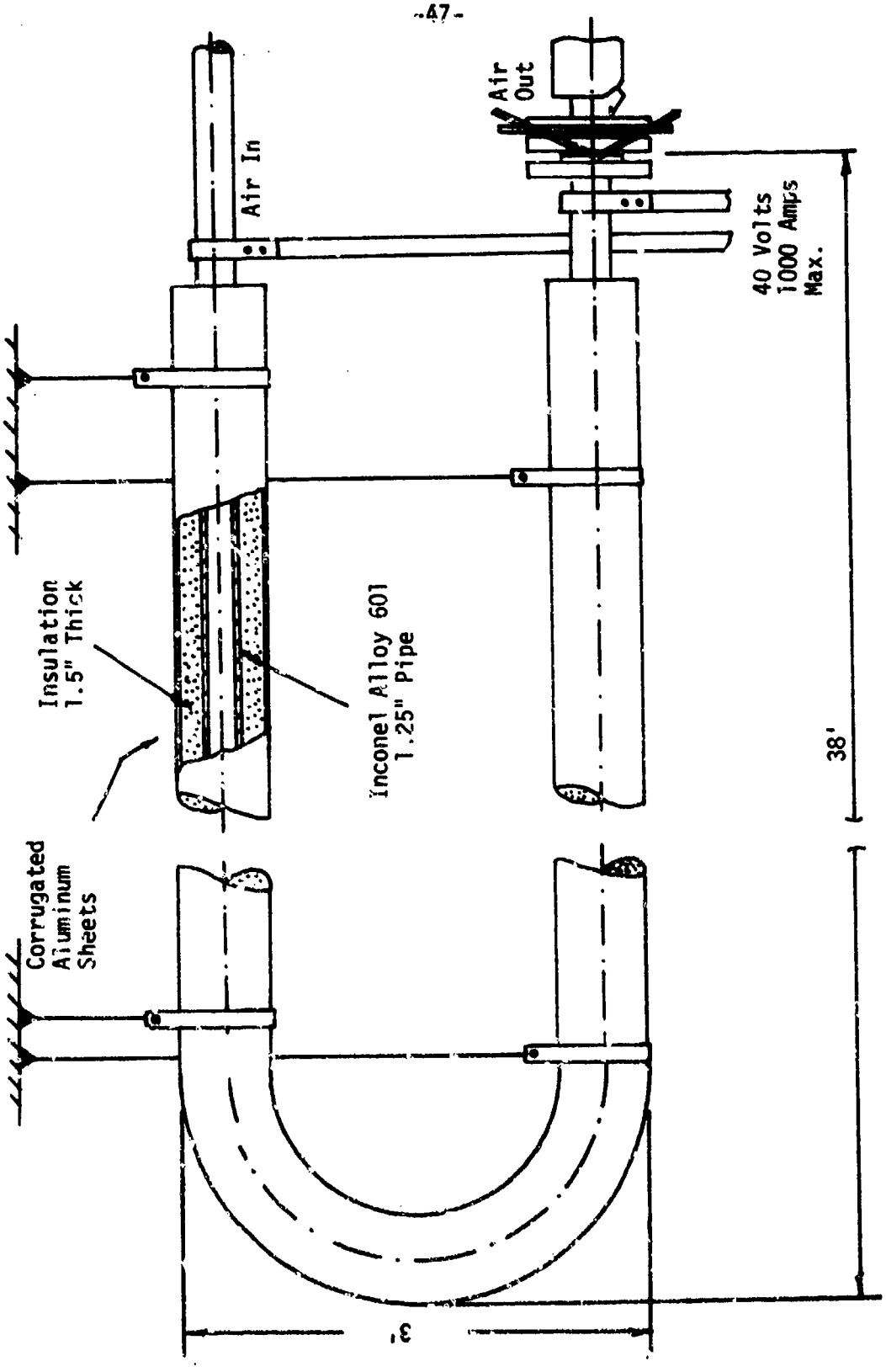

Figure 9: Details of the Heated Air Facility

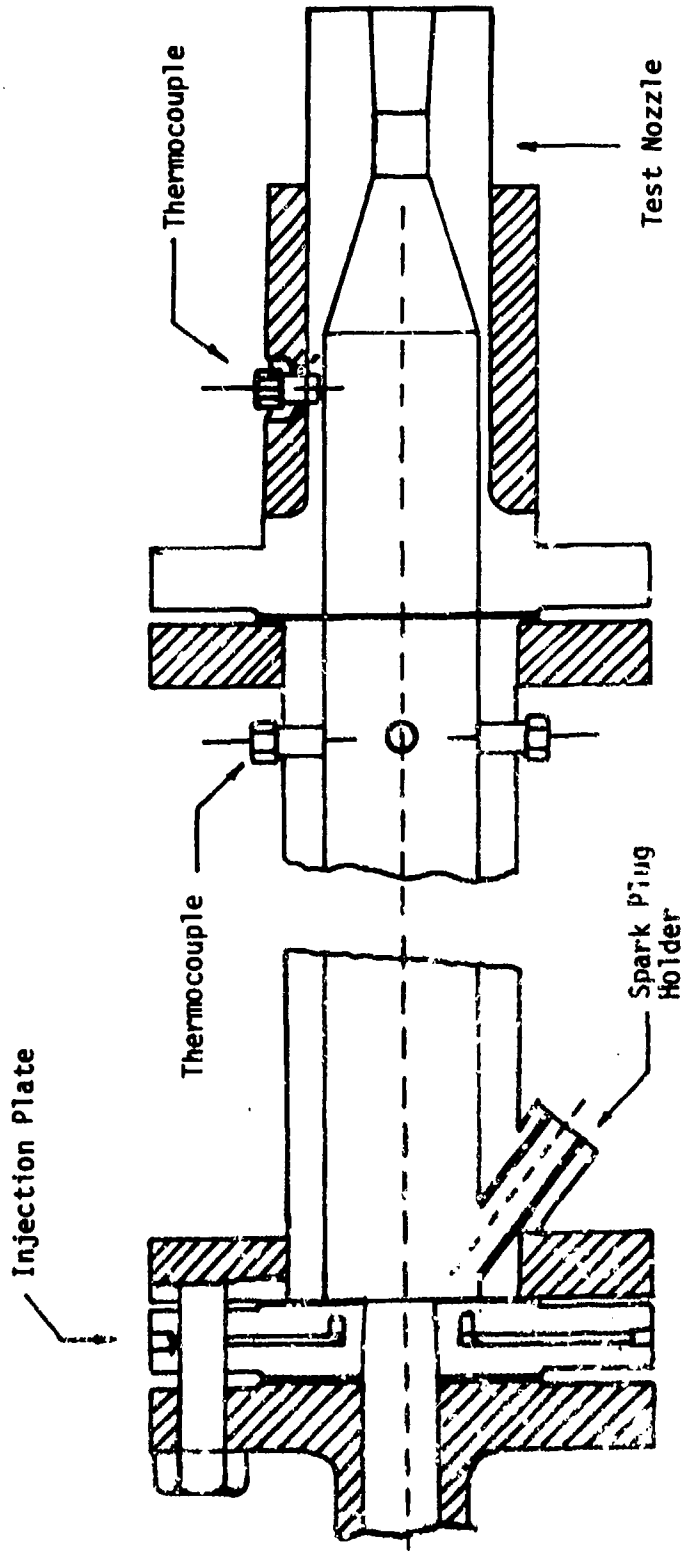

Figure 10: Cross-Section of Gas-Fired Pre-Burner

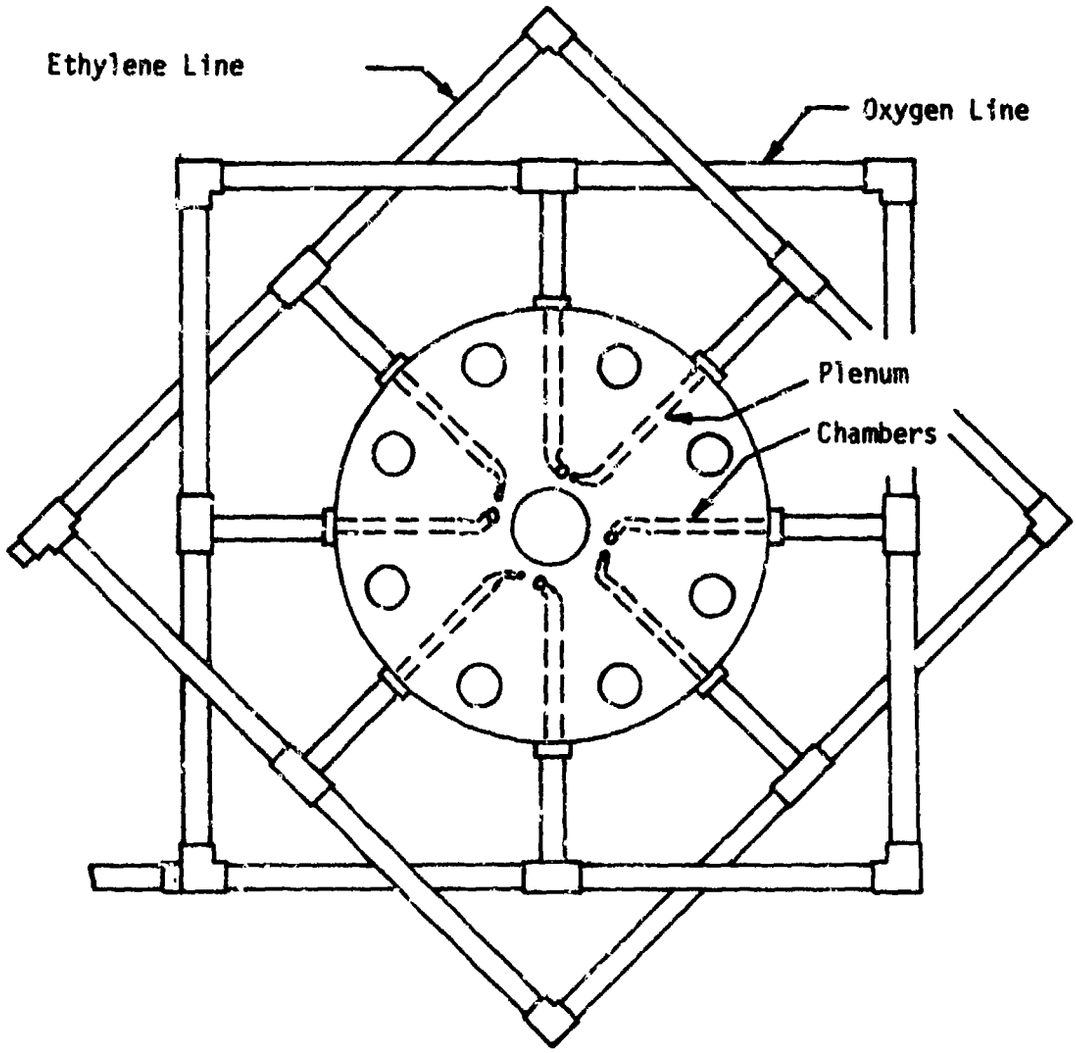

1. Flange 6.5" Diam. S.S.
2. All Tubing .375" Diam. S.S.
3. All Plenum Chambers .25" Diam.
4. Ethylene Exit Holes .0313" Diam.
5. Oxygen Exit Holes .0625" Diam.
6. Center Hole .9" Diam.

Figure 11: Cross-Section of Injector Plate for Gas-Fired Pre-Burner

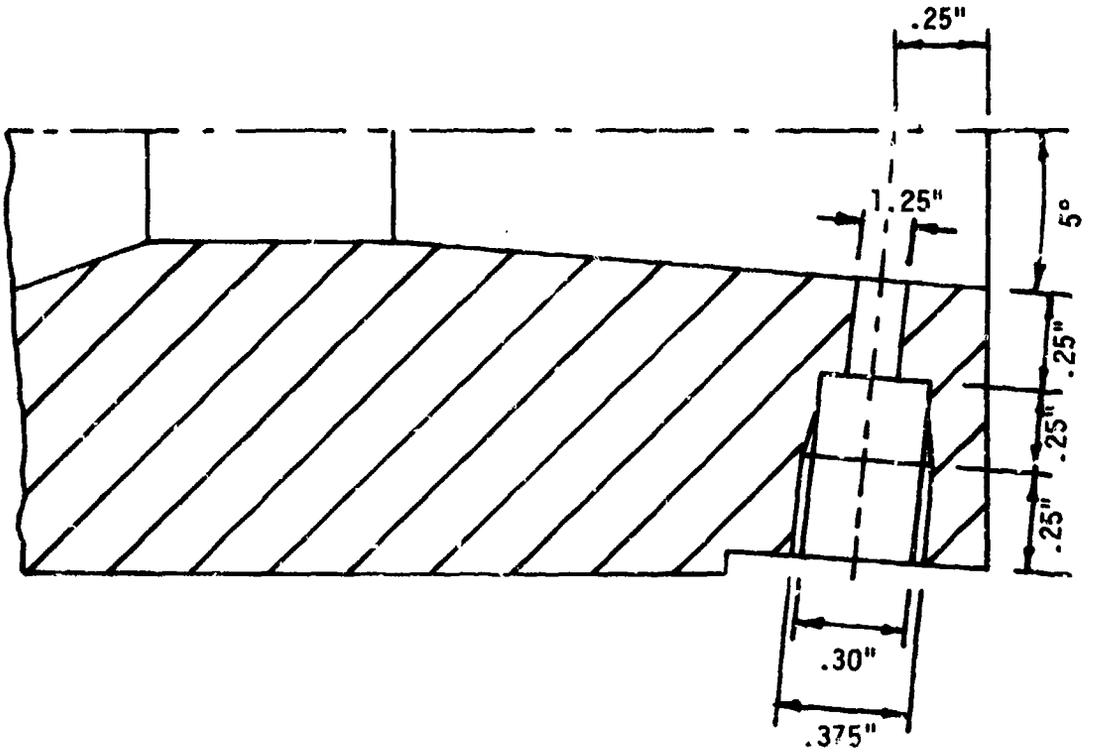

Insert Containing Thermocouple

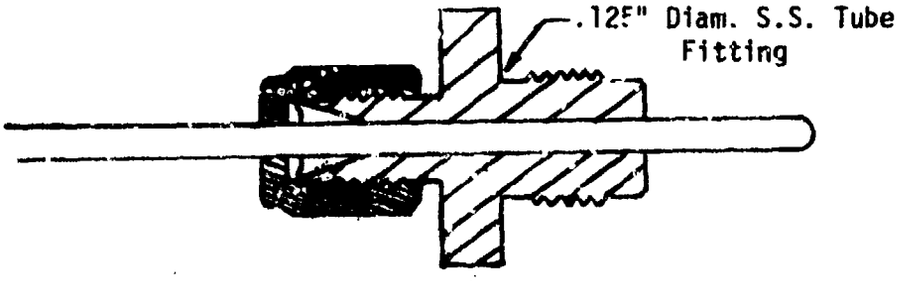

Figure 12: Wall Temperature Instruments

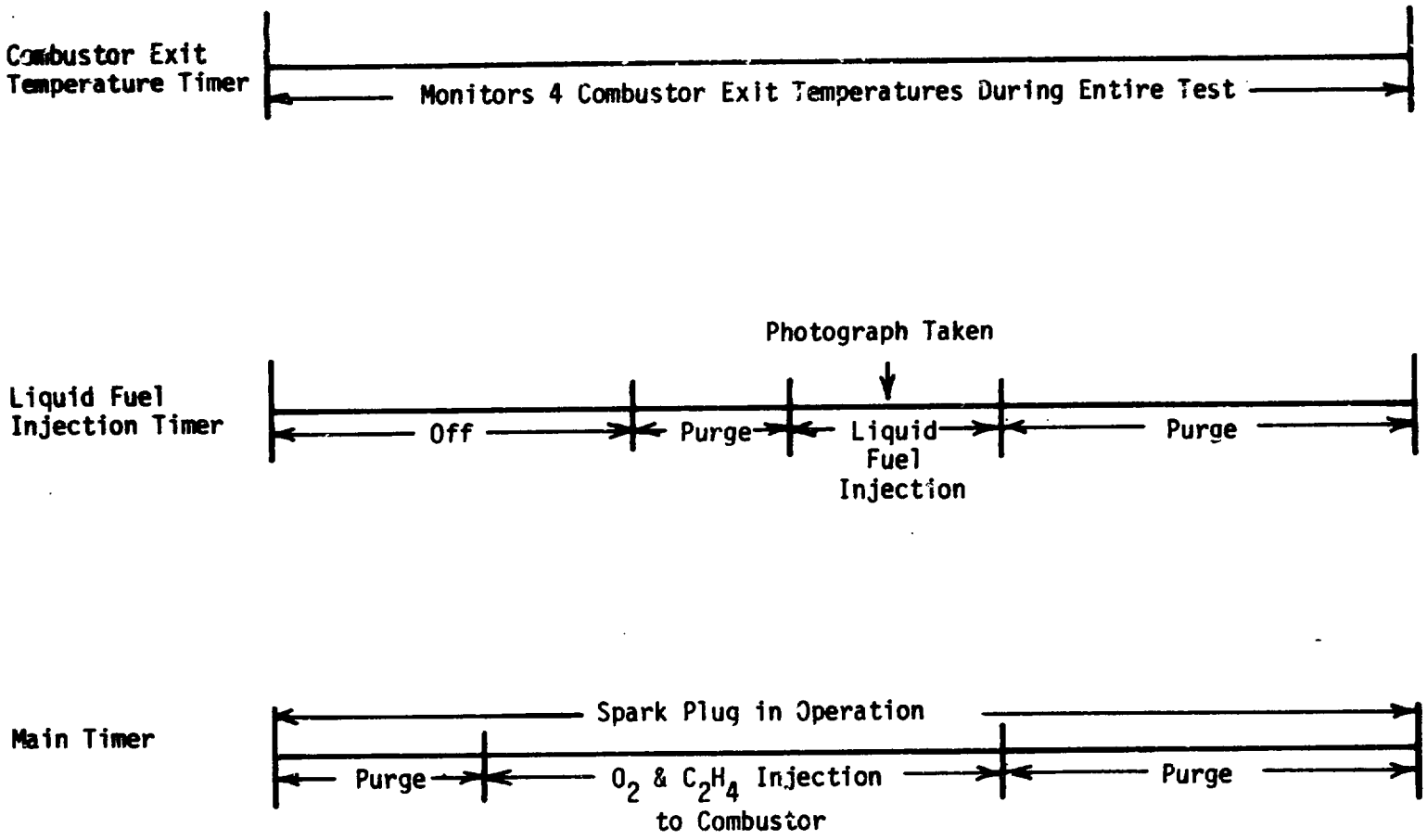

Figure 13: Schematic of Timer Sequences

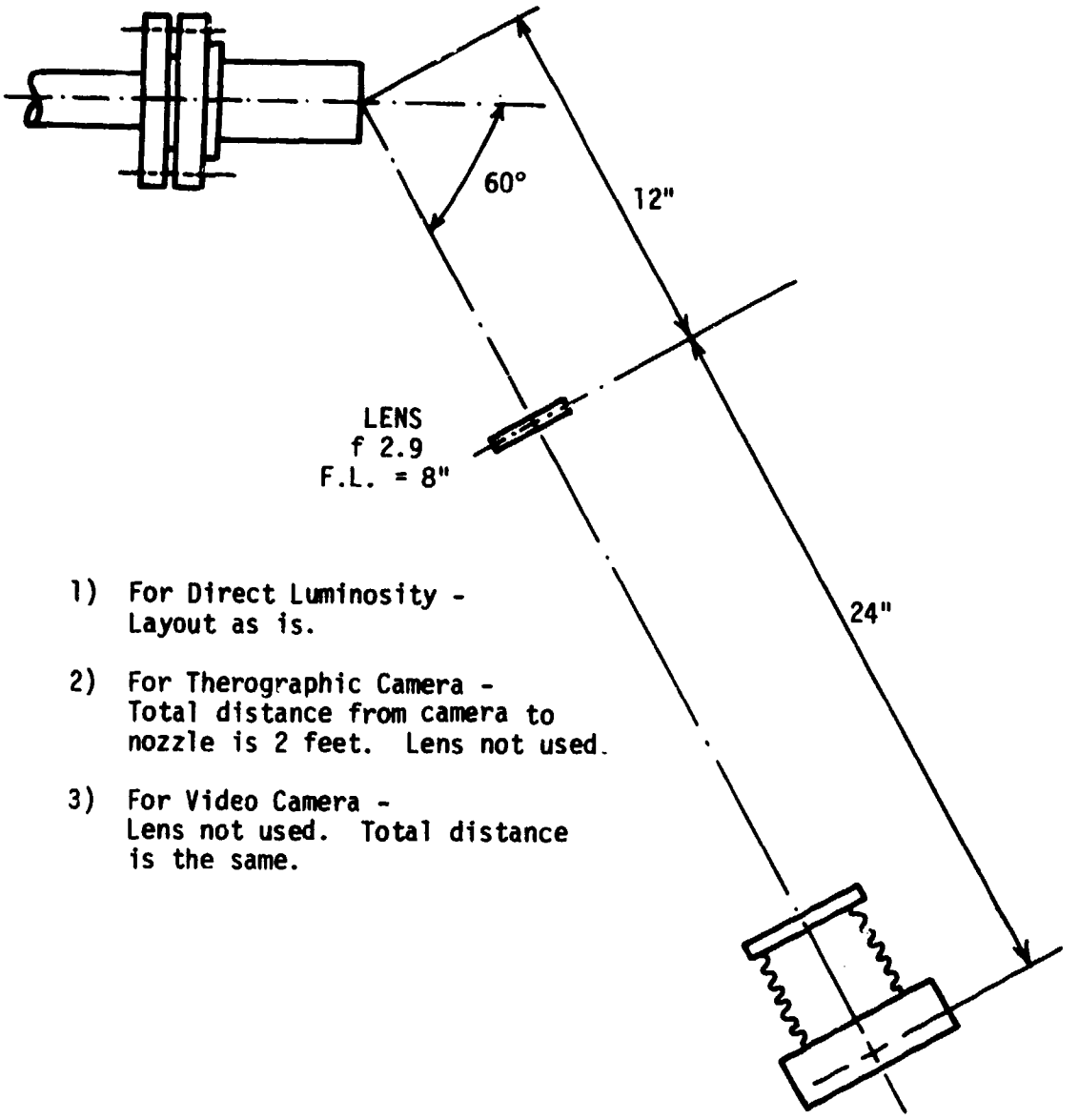

1) For Direct Luminosity -
Layout as is.

2) For Therographic Camera -
Total distance from camera to nozzle is 2 feet. Lens not used.

3) For Video Camera -
Lens not used. Total distance is the same.

Figure 14: Layout for Optical Observations

a. Water, T_o = 1774 °F, P_{inj} = 135 psi

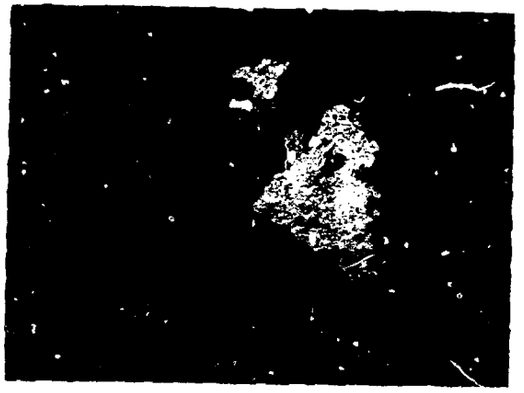

b. Kerosene, T_o = 1751 °F, P_{inj} = 135 psi

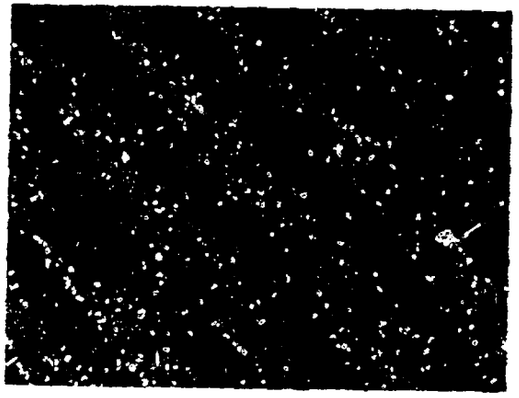

c. Water, T_o = 2079 °F, P_{inj} = 135 psi

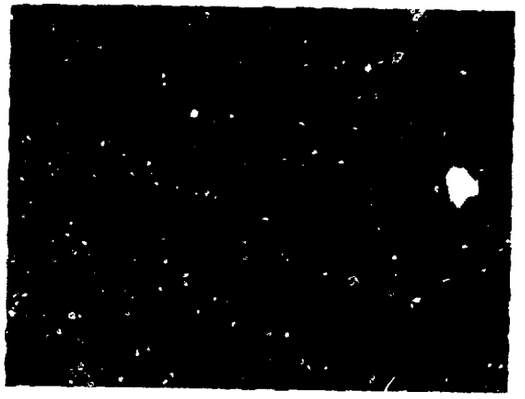

d. Kerosene, T_o = 2091 °F, P_{inj} = 135 psi

Figure 15: Direct Luminosity Photographs of Water, Kerosene and CS_2 Injected Transverse

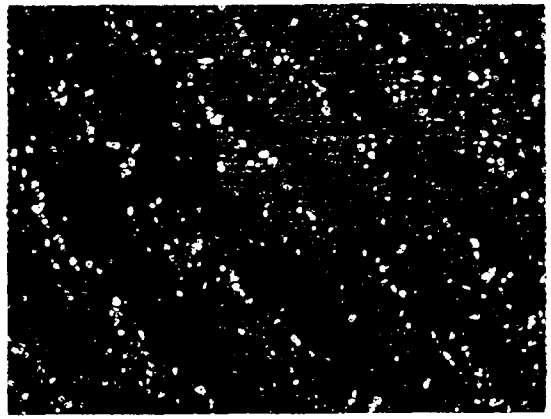

a. T_o = 1950 °F, P_{inj} = 135 psi

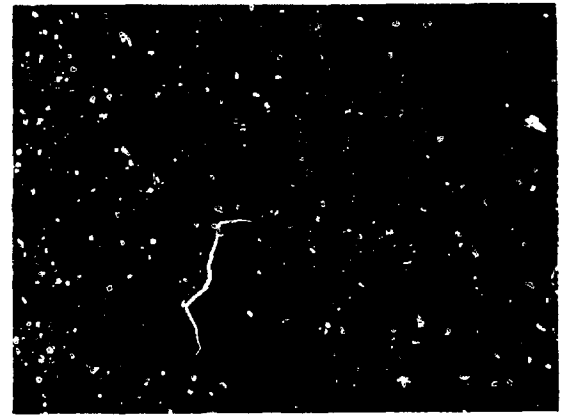

b. T_o = 2055 °F, P_{inj} = 135 psi

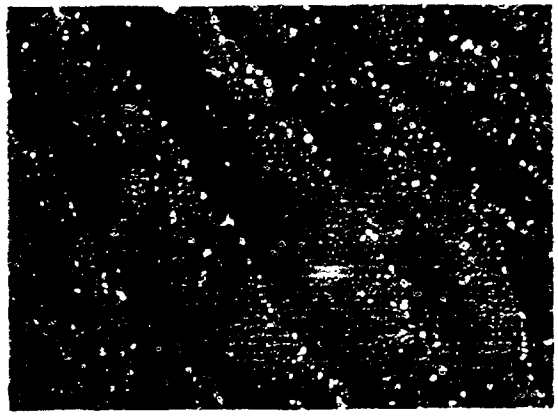

c. T_o = 2115 °F, P_{inj} = 135 psi

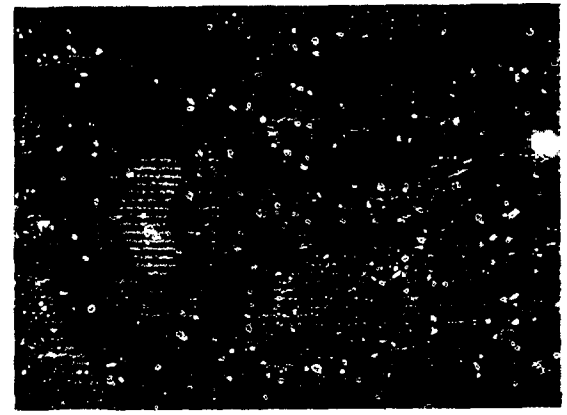

d. T_o = 2200 °F, P_{inj} = 135 psi

Figure 16: Infrared Photographs of Kerosene Injected Transverse

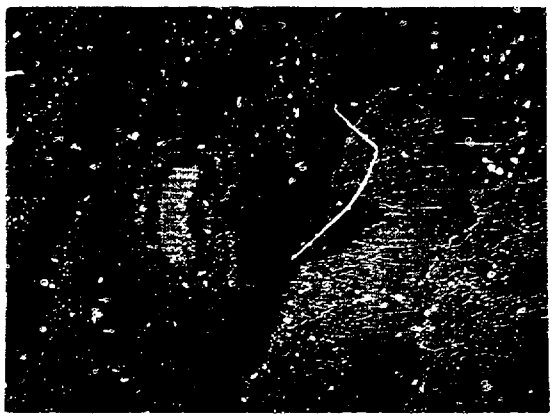

a. P_{inj} = 135 psi, T_o = 2200 °F

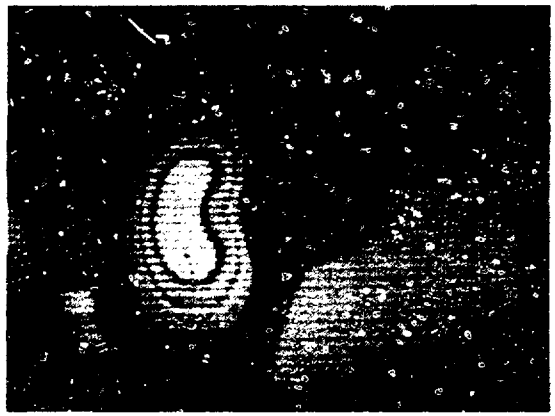

b. P_{inj} = 300 psi, T_o = 2200 °F

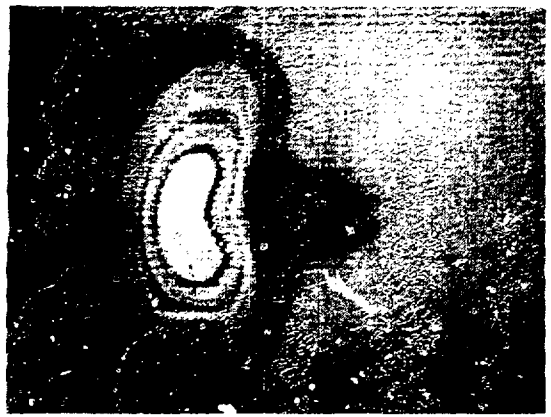

c. P_{inj} = 450 psi, T_o = 2200 °F

Figure 17: Infrared Photographs of Water Injected Transverse at Various Pressures

a. P_{inj} = 135 psi, T_o = 2151 °F

b. P_{inj} = 300 psi, T_o = 2151 °F

c. P_{inj} = 450 psi, T_o = 2151 °F

Figure 18: Infrared Photographs of Kerosene Injected Transverse at Various Pressures

a. P_{inj} = 135 psi, T_o = 2200 °F

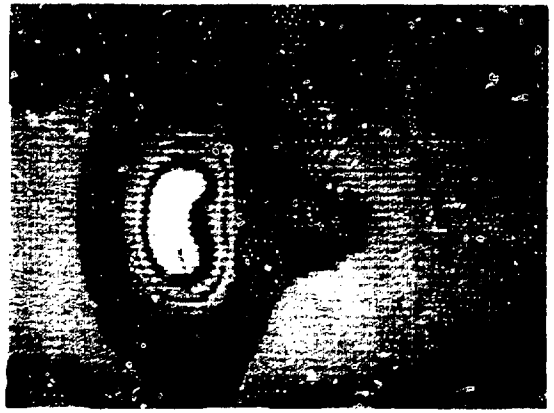

b. P_{inj} = 300 psi, T_o = 2200 °F

c. P_{inj} = 450 psi, T_o = 2200 °F

Figure 19: Infrared Photographs of CS_2 Injected Transverse at Various Pressures

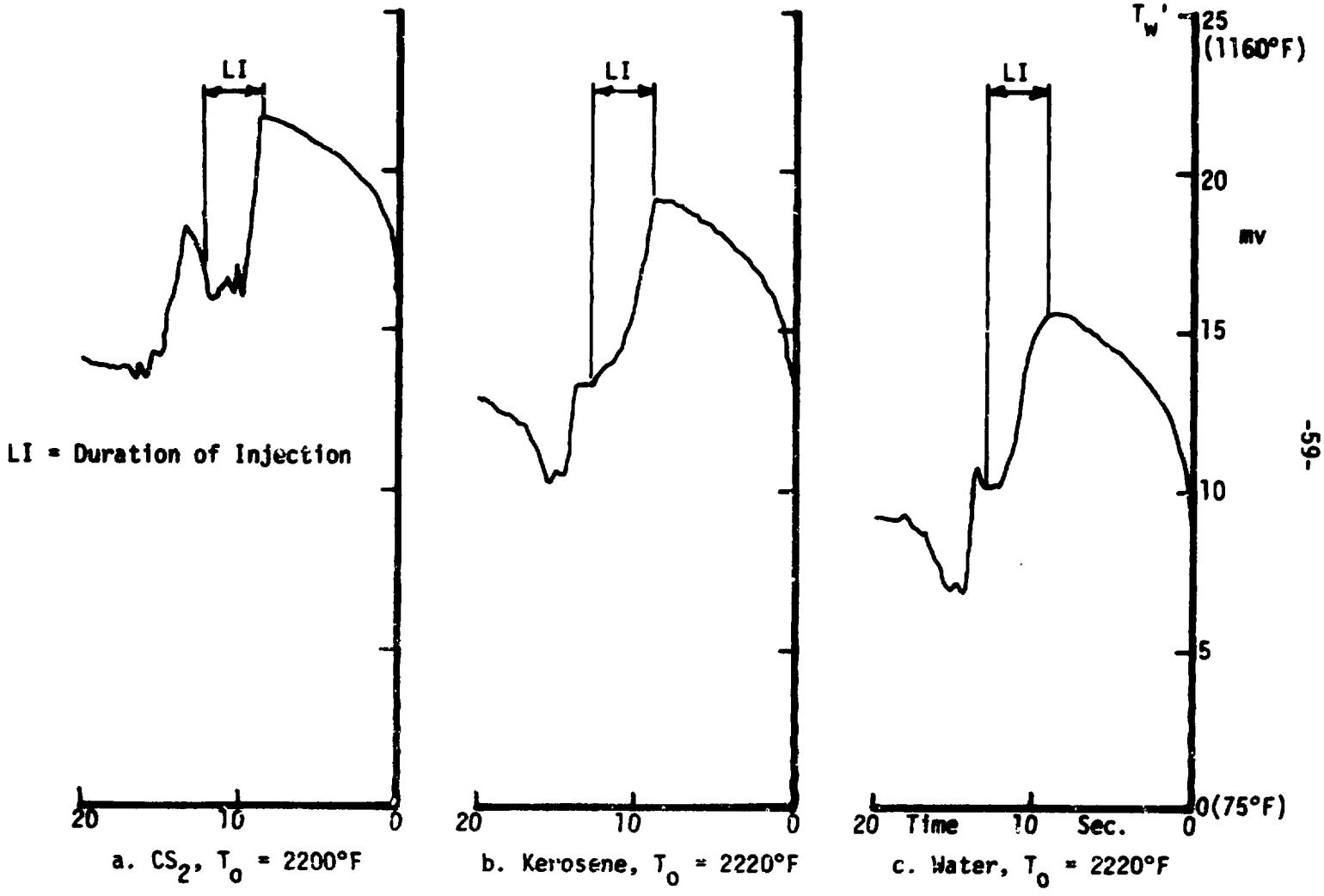

Figure 20: Wall Temperature Tracings of Normal Injection of CS_2, Kerosene and Water at 135 psi

a. T_o = 2007 °F, P_{inj} = 135 psi

b. T_o = 2042 °F, P_{inj} = 135 psi

c. T_o = 2103 °F, P_{inj} = 135 psi

Figure 21: Infrared Photographs of Water Injected Upstream

a. T_o = 2007 °F, P_{inj} = 135 psi

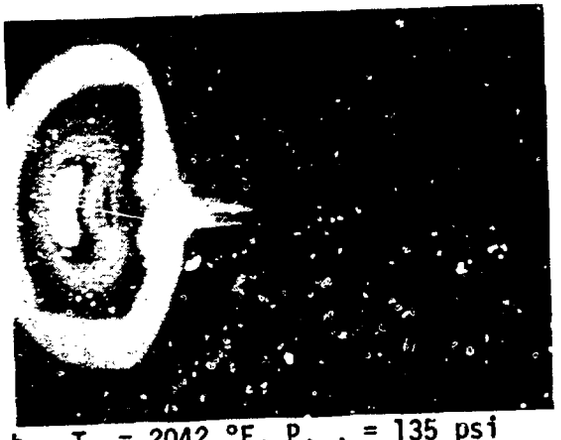

b. T_o = 2042 °F, P_{inj} = 135 psi

c. T_o = 2139 °F, P_{inj} = 135 psi

Figure 22: Infrared Photographs of Kerosene Injected Upstream

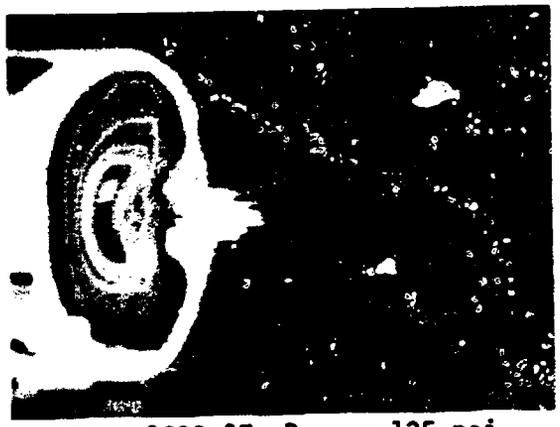

a. T_o = 1983 °F, P_{inj} = 135 psi

b. T_o = 2030 °F, P_{inj} = 135 psi

c. T_o = 2127 °F, P_{inj} = 135 psi

Figure 23: Infrared Photographs of CS_2 Injected Upstream

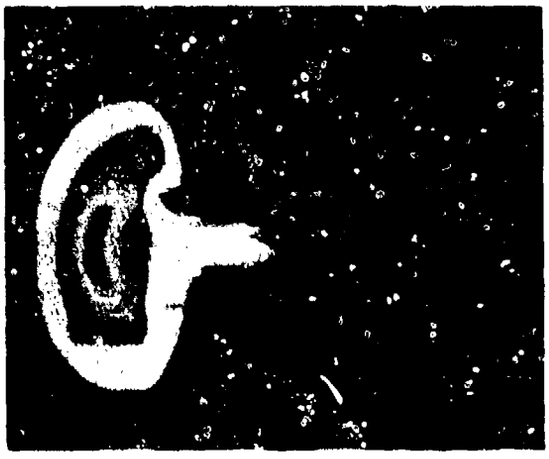

a. P_{inj} = 300 psi, T_o = 2288 °F

b. P_{inj} = 450 psi, T_o = 2263 °F

Figure 24: Infrared Photographs of Water Injected Upstream at Different Pressures

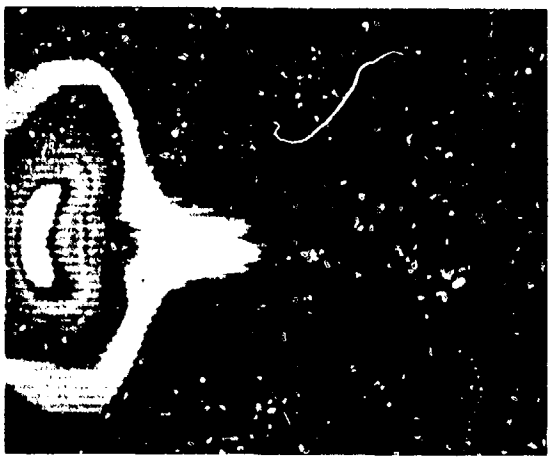

a. P_{inj} = 300 psi, T_o = 2238 °F

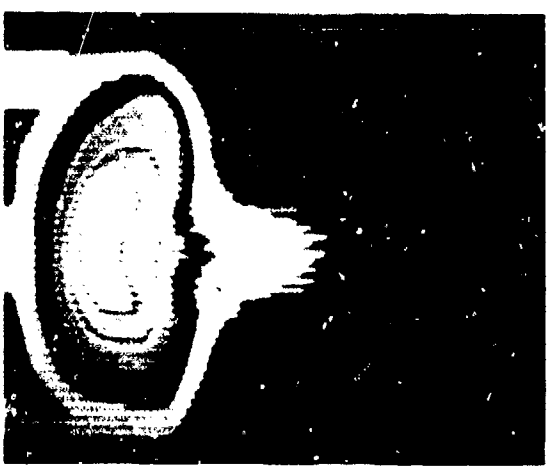

b. P_{inj} = 450 psi, T_o = 2251 °F

Figure 25: Infrared Photographs of Kerosene Injected Upstream at Different Pressures

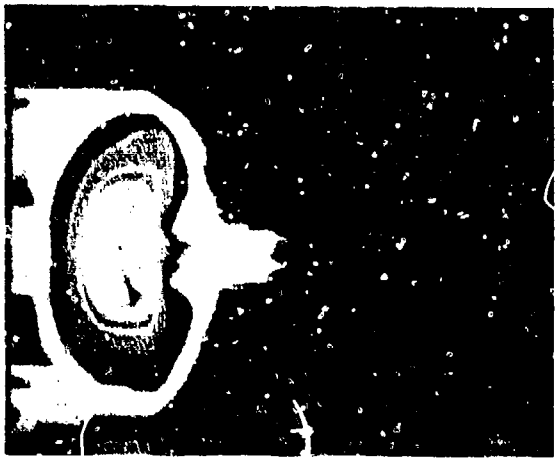

a. P_{inj} = 300 psi, T_o = 2213 °F

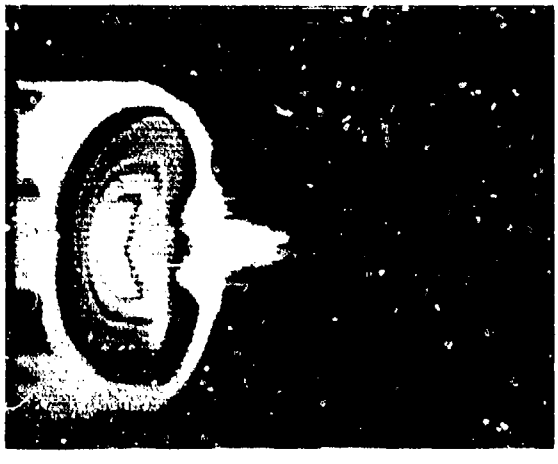

b. P_{inj} = 450 psi, T_o = 2213 °F

Figure 26: Infrared Photographs of CS_2 Injected Upstream at Different Pressures

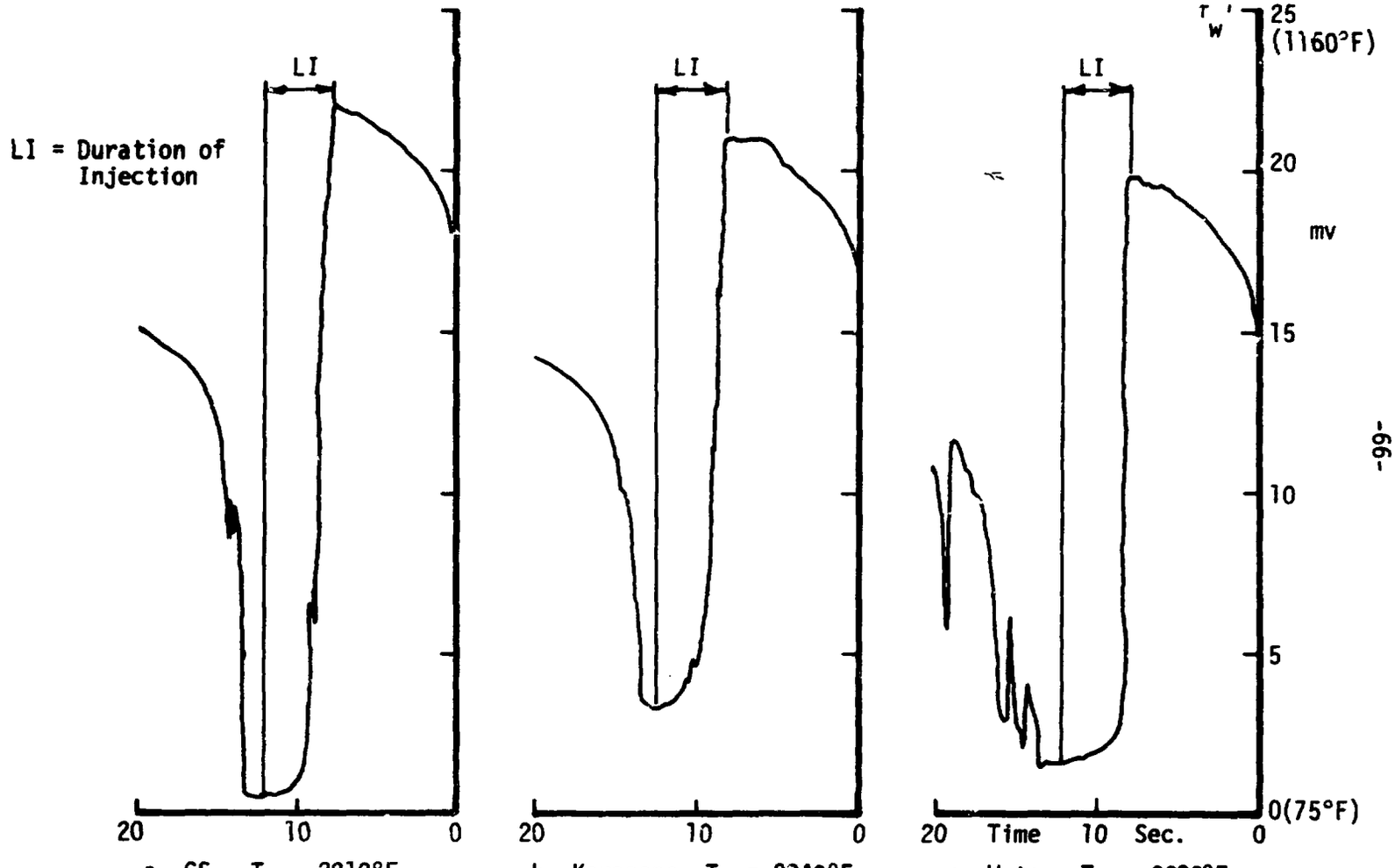

a. CS_2, T_o - 2210°F b. Kerosene, T_o = 2240°F c. Water, T_o = 2290°F

Figure 27: Wall Temperature Tracings of Upstream Injection CS_2, Kerosene and Water at 300 psi

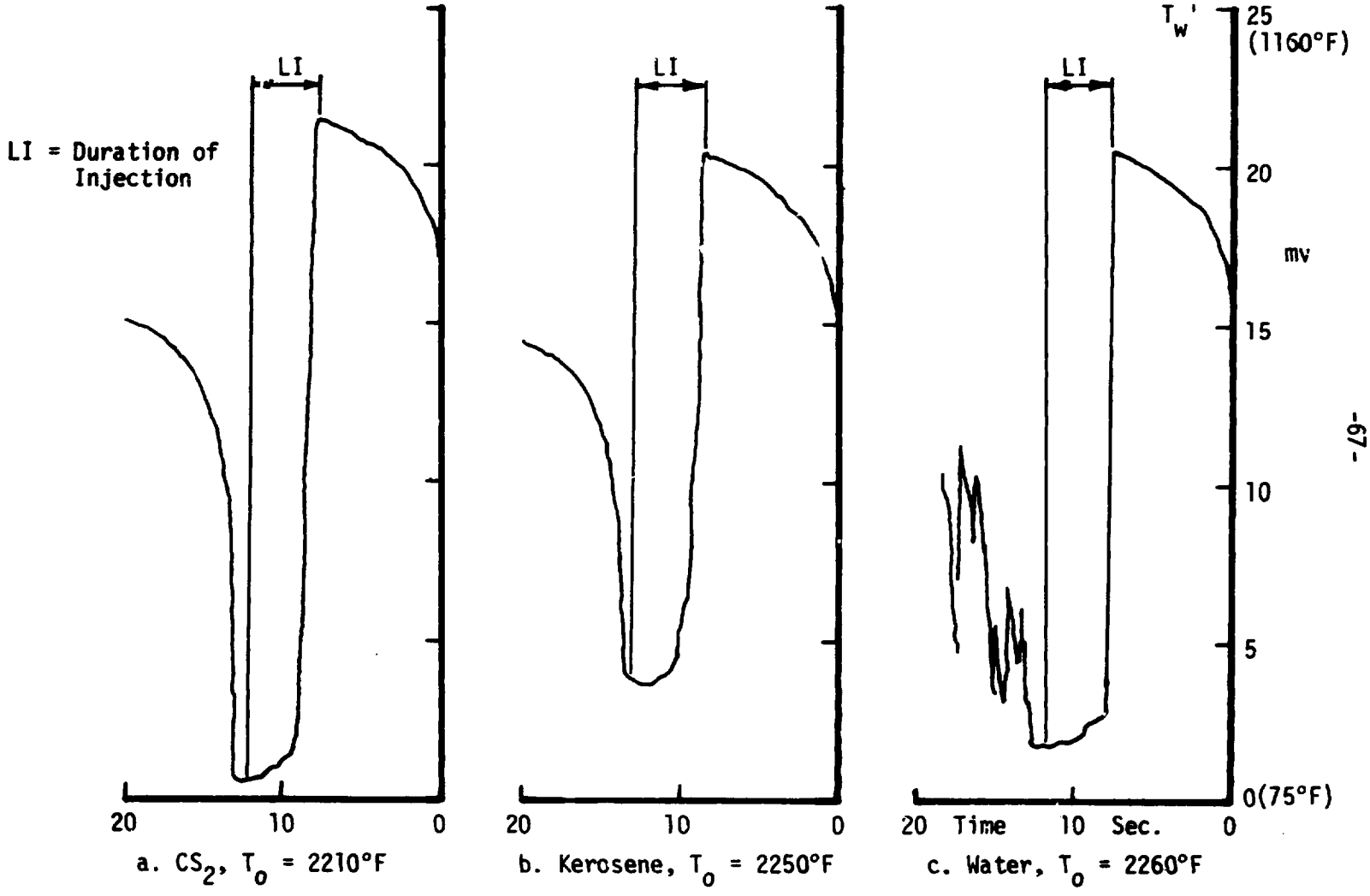

Figure 28: Wall Temperature Tracings of Upstream Injection of CS_2, Kerosene and Water at 450 psi

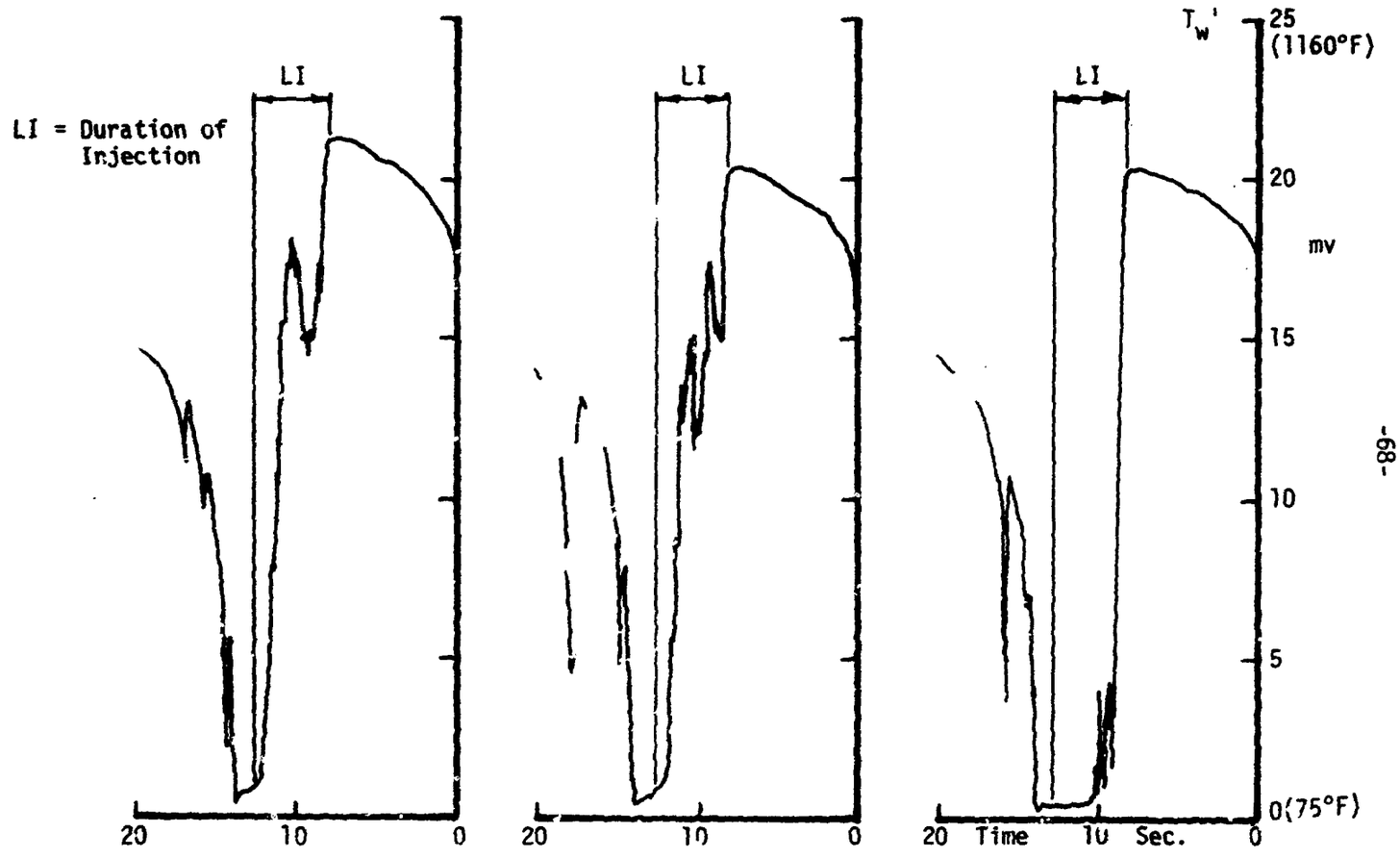

a. T_o = 2130°F, P_{inj} = 135 psi b. T_o = 2030°F, P_{inj} = 135 psi c. T_o = 1980°F, P_{inj} = 135 psi

Figure 29: Wall Temperature Tracings of CS_2 Injected Upstream at Various Stagnation Temperatrues

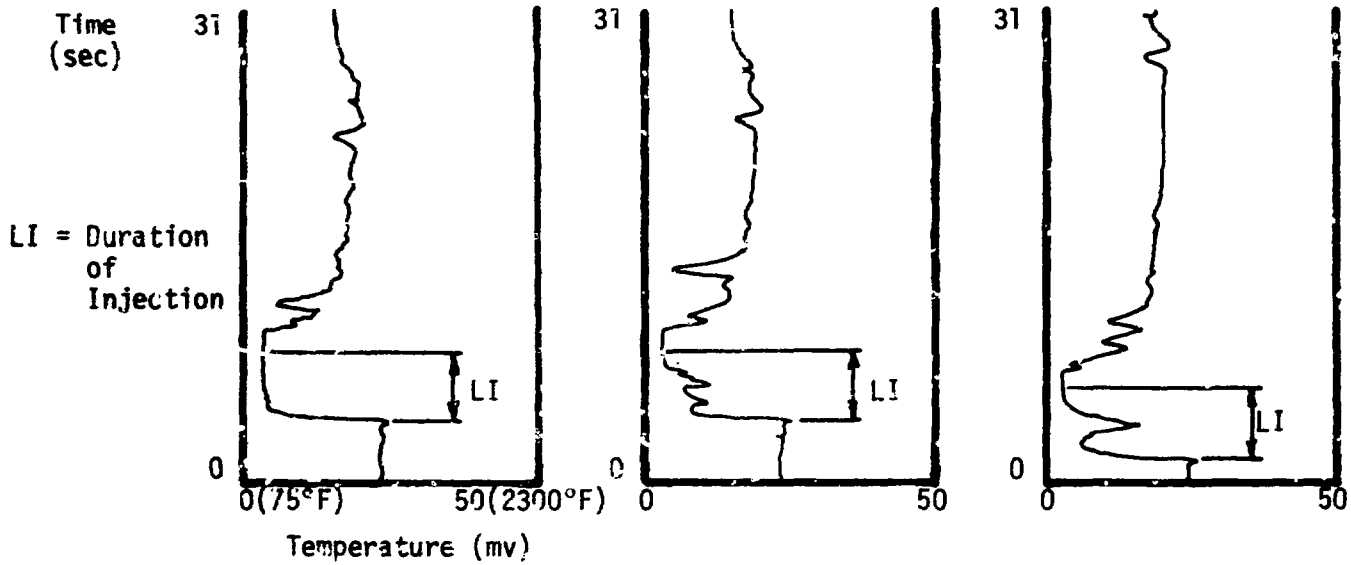

a. T_o = 1980°F, P_{inj} = 135 psi

b. T_o = 2030°F P_{inj} = 135 psi

c. T_o = 2130°F P_{inj} = 135 psi

Figure 30: In-Flow Temperature Tracings of Upstream Injection of CS_2 at Various Pressures

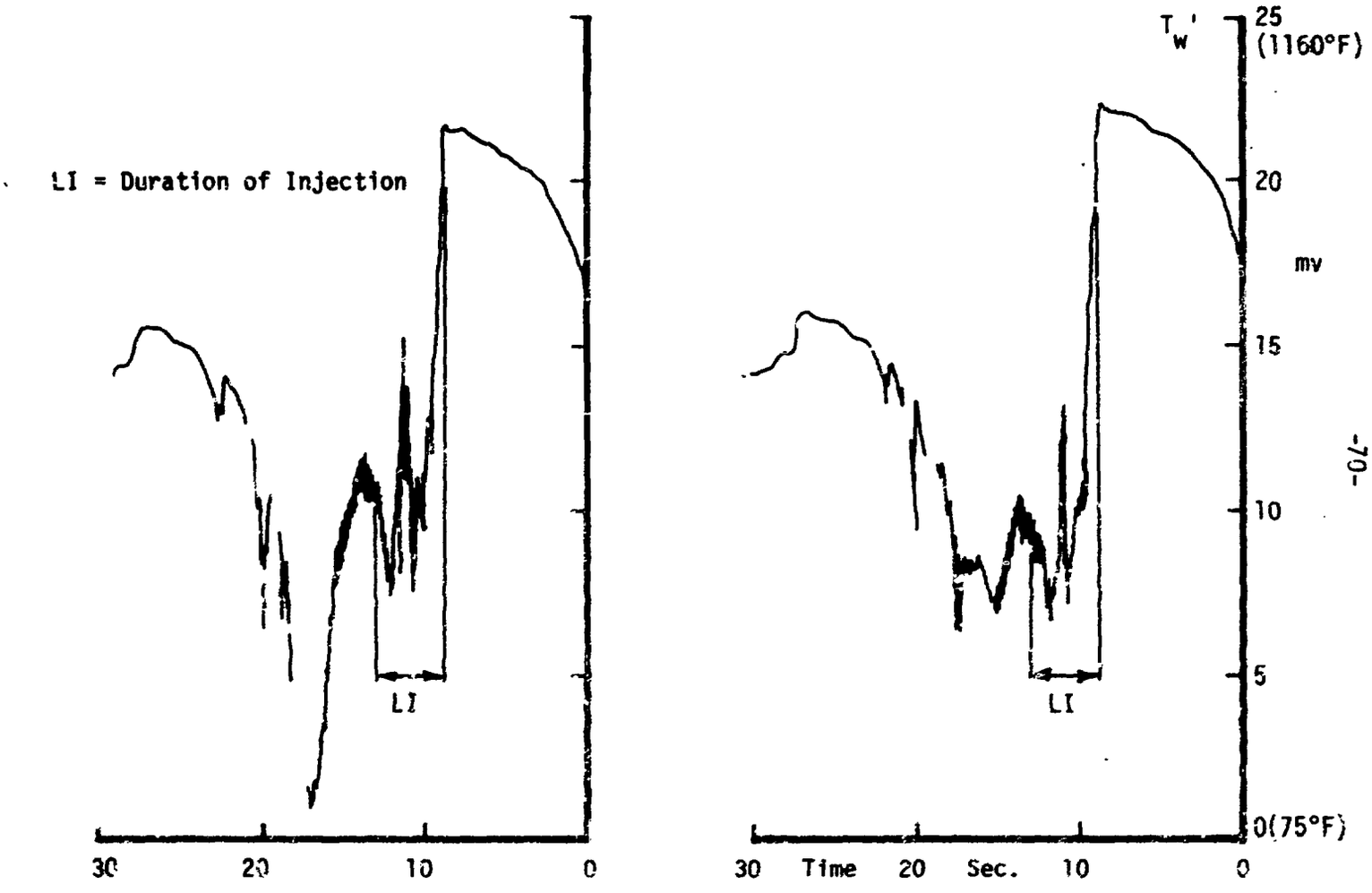

a. P_{inj} = 80 psi, T_o = 2210°F

b. P_{inj} = 90 psi, T_o = 2210°F

Figure 31: Wall Temperature Tracings of CS_2 at Low Upstream Injection Pressures

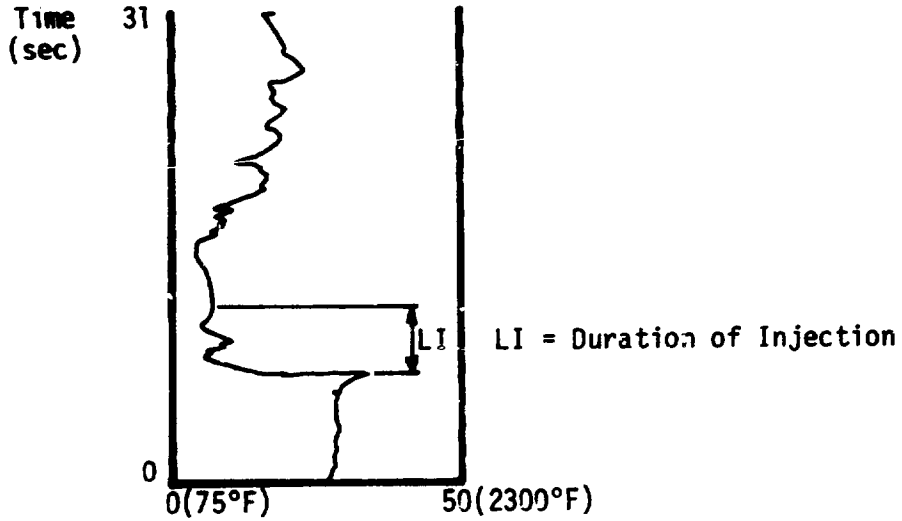

a. P_{inj} = 80 psi, T_o = 2210°F

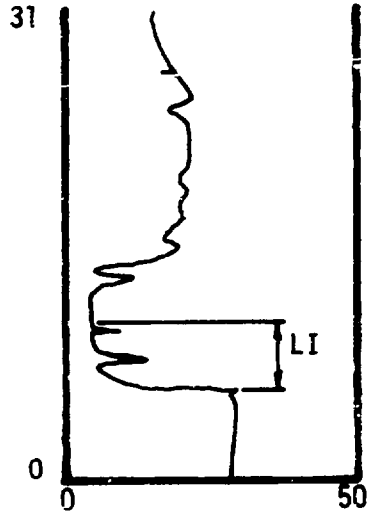

b. P_{inj} = 90 psi, T_o = 2210°F

Figure 32: In-Flow Temperature Tracings of Upstream Injection of CS_2 at Various Pressures

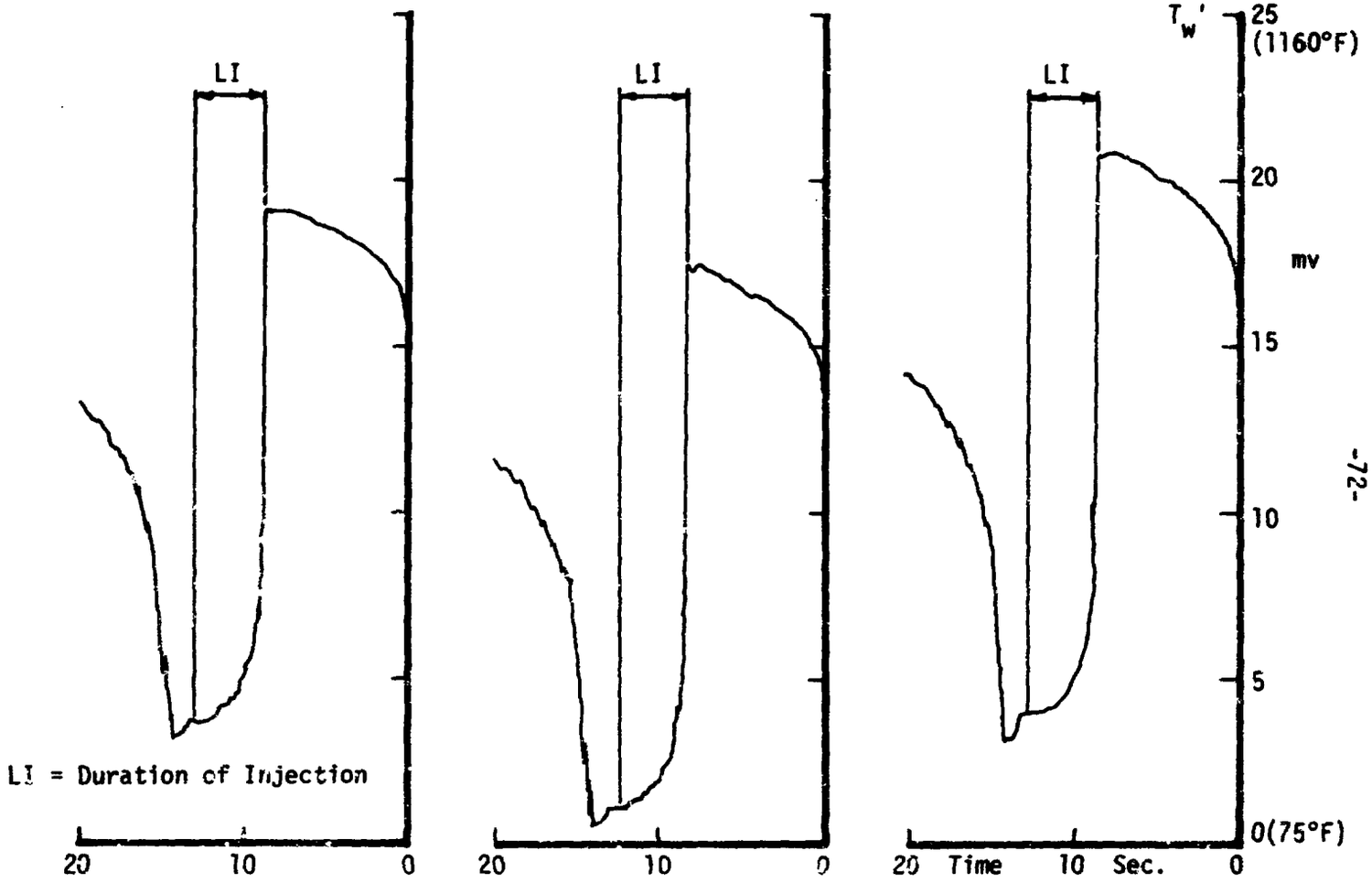

a. T_o = 2040°F, P_{inj} = 135 psi b. T_o = 2040°F, P_{inj} = 135 psi c. T_o = 2140°F, P_{inj} = 135 psi

Figure 33: Wall Temperature Tracings of Kerosene Injected Upstream at Various Stagnation Temperatures